Yield stress effects on Rayleigh–Bénard convection

By J. ZHANG[1], D. VOLA[2] AND I. A. FRIGAARD[1,3]†

[1]Department of Mathematics, University of British Columbia, 1984 Mathematics Road,
Vancouver, BC, V6T 1Z2, Canada

[2]Institut de Radioprotection et de Sûreté Nucléaire (IRSN), BP3-13115,
St Paul-lez-Durance CEDEX, France

[3]Department of Mechanical Engineering, University of British Columbia,
2054-6250 Applied Science Lane, Vancouver, BC, Canada, V6T 1Z4

We examine the effects of a fluid yield stress on the classical Rayleigh–Bénard instability between heated parallel plates. The focus is on a qualitative characterization of these flows, by theoretical and computational means. In contrast to Newtonian fluids, we show that these flows are linearly stable at all Rayleigh numbers, Ra, although the usual linear modal stability analysis cannot be performed. Below the critical Rayleigh number for energy stability of a Newtonian fluid, Ra_E, the Bingham fluid is also globally asymptotically stable. Above Ra_E, we provide stability bounds that are conditional on $Ra - Ra_E$, as well as on the Bingham number B, the Prandtl number Pr, and the magnitude of the initial perturbation. The stability characteristics therefore differ considerably from those for a Newtonian fluid. A second important way in which the yield stress affects the flow is that when the flow is asymptotically stable, the velocity perturbation decays to zero in a finite time. We are able to provide estimates for the stopping time for the various types of stability. A consequence of the finite time decay is that the temperature perturbation decays on two distinctly different time scales, i.e. before/after natural convection stops. The two decay time scales are clearly observed in our computational results.

We are also able to determine approximate marginal stability parameters via computation, when in the conditional stability regime, although computation is not ideal for this purpose. When just above the marginal stability limits, perturbations grow into a self-sustained cellular motion that appears to resemble closely the Newtonian secondary motion, i.e. Rayleigh–Bénard cells. When stable, however, the decaying flow pattern is distinctly different to that of a Newtonian perturbation. As $t \to \infty$, a stable Newtonian perturbation decays exponentially and asymptotically resembles the least stable eigenfunction of the linearized problem. By contrast, as t approaches its stopping value, the Bingham fluid is characterized by growth of a slowly rotating (almost) unyielded core within each convection cell, with fully yielded fluid contained in a progressively narrow layer surrounding the core. Finally, preliminary analyses and remarks are made concerning extension of our results to inclined channels, stability of three-dimensional flows and the inclusion of residual stresses in the analysis.

1. Introduction

Non-Newtonian fluids occur in a very broad range of industrial and natural flows, ranging from polymer processing, the construction of oil wells, processing of foodstuffs to lava and mud flows. The term non-Newtonian is all-encompassing and describes various different effects. For a great many fluids and flow situations, the principal deviation from Newtonian behaviour manifests in a nonlinear dependence of shear rate on the rate of strain (see e.g. Bird, Armstrong & Hassager 1987, §2.2). Such fluids are termed generalized Newtonian fluids. Two key phenomenological effects are: (i) shear-thinning/thickening (i.e. the viscosity may decrease or increase with rate of strain); (ii) fluids may exhibit a yield stress (i.e. below a certain shear stress there is a zero strain rate), and these are termed visco-plastic fluids. Often, generalized Newtonian behaviour is further complicated by other effects, e.g. thixotropy, visco-elasticity, elastic creep below the yield stress. However, there are still wide parameter ranges in which the shear rheology described by a generalized Newtonian model is a good description and such models are consequently used widely in industrial and geophysical applications.

This paper considers the onset of natural convection for a yield stress fluid in the Rayleigh–Bénard context. Such fluids were first considered by Bingham (1922), after whom the most commonly used model is named. Later Bingham fluids were studied more extensively by Oldroyd (1947), Prager (1954), Mossolov & Miasnikov (1965, 1966) and by Duvaut & Lions (1976). Different yield stress materials and an overview of the known analytical solutions to the Navier–Stokes equations for yield-stress fluids were presented in the review by Bird, Dai & Yarusso (1983). Slightly more complex visco-plastic models are the Herschel–Bulkley and Casson models.

There appears to be no study of Rayleigh–Bénard convection for Bingham fluids in the literature. At the outset this is surprising given the wide occurrence of such fluids in application areas where natural convection is important, e.g. geophysics (magma/mantle convection), chocolate manufacture (and many other less palatable food products that have yield stresses), pulp processing and drying, oilfield cementing and drilling, the flow of heavy oils in porous media, construction cementing, nuclear safety, baking. The lack of attention to the problem is easier to understand once the key difficulty is understood. Simplistically, a yield stress fluid is a fluid with an effective viscosity $\hat{\eta}$, given by:

$$\hat{\eta} = \hat{\mu} + \frac{\hat{\tau}_Y}{\hat{\gamma}},$$

where $\hat{\mu}$ and $\hat{\tau}_Y$ are, respectively, the plastic viscosity and yield stress of the fluid; the rate of strain is denoted $\hat{\gamma}$. In the Rayleigh–Bénard paradigm, the base flow is static, with zero rate of strain and hence the effective viscosity is infinite everywhere. If we follow the classical approach of linear stability, we have to perturb about a fluid with infinite effective viscosity which is obviously problematic.

For other purely viscous generalized Newtonian fluids (e.g. power-law fluids, Carreau fluids, etc.), the same problem does not exist. Similarly, for visco-elastic fluids it is possible to progress by classical linear stability. Much of the study of Rayleigh–Bénard convection for Newtonian (and these other) fluids is based on linear modal theories (e.g. onset, weakly nonlinear perturbations, pattern formation). Therefore, the lack of a linear modal theory for yield stress fluids is a major handicap, and probably explains why the problem has not been studied. Once we understand this barrier, it becomes clear that other methods must be employed, and here we use the only two

methods that appear to be applicable for the problem: energy stability theory and numerical simulation.

Therefore, although a generalized Newtonian fluid is one of the simplest non-Newtonian models and although the Bingham fluid is the simplest yield stress fluid to study, the Rayleigh–Bénard stability problem is arguably much harder to study than for 'more complex' non-Newtonian fluids. Our aims for the paper are consequently more modest than might be expected when studying the Rayleigh–Bénard paradigm. First, we aim to understand qualitatively the nature of the stability of the base state, for a fluid with a finite yield stress. For example, although there is no classical linear stability eigenvalue problem, is the flow still stable or unstable to sufficiently small perturbations and how is the stability characterized? Secondly, we would like to demonstrate computationally that there are indeed convective instabilities in these flows, above certain instability thresholds.

There is much literature on the Rayleigh–Bénard problem for Newtonian fluids, and numerous interesting extensions; see, for example, Koschmieder (1993) for an overview and review. Rayleigh–Bénard convection has also been studied for various viscous and visco-elastic non-Newtonian fluids (e.g. Khayat 1995*a–c*, 1996; Martinez-Mardones, Tiemann & Walgraef 1999, 2000; Park & Ryu 2001*a,b*; Abu-Ramadan, Hay & Khayat 2003), but not for yield stress fluids. Discarding the issue of stability/onset, one can also find various studies of forced and natural convection with yield stress fluids (e.g. Round & Yu 1993; Nouar, Devienne & Lebouche 1994; Patel & Ingham 1994; Soares *et al.* 1999, 2003).

A key property of yield stress fluid flows is that static steady-state solutions are frequently both nonlinearly stable and exhibit decay of the perturbations in a finite time. This was first demonstrated for the case of a one-dimensional duct flow by Glowinski, Lions & Trémolières (1981) and Glowinski (1984). Finite time decay results are also proved straightforwardly for various viscometric flows for which the yield limits are known (see e.g. Huilgol, Mena & Piau 2002). In the different physical context of nonlinear diffusion filtering in image processing (but with analogous mathematics), visco-plastic stopping time estimates have been used within a multiple scales framework, to predict when noise is optimally removed from an image (see Frigaard, Ngwa & Scherzer 2003).

In this paper, we extend finite time decay results to a much broader class of flows, namely those with temperature coupling via buoyancy. Although focused at the Rayleigh–Bénard problem, this serves as a model problem for a much wider range of practically relevant applications. The implication of a finite time decay is that thermal convection stops after a certain known time. This has particular relevance for the design of 'smart' thermal switching devices, in which the heat transfer may be switched on/off by control of the yield stress magnitude, for example, by use of electro-rheological or magneto-rheological fluids, (typically the conductive heat flux across the Rayleigh–Bénard cell will be significantly smaller than the convective heat flux). The idea of controlling Rayleigh–Bénard convection for Newtonian fluids is not new. There has been extensive study over many years by Bau, Tang and latterly Howle (and their co-workers), which is focused at feedback and active control of Rayleigh–Bénard convection via a variety of methods (e.g. Singer & Bau 1991; Tang & Bau 1993, 1994, 1996; Howle 1997, 2000; Wagner, Bertozzi & Howle 2003). However, apart from the notion of flow control and control theory methodology (which we do not deal with here), these lend little to our study.

Finally, we note that finite time decay is limited to static stability of yield stress fluids. There have been various studies of the hydrodynamic stability of yield stress

fluids, usually Bingham fluids, in configurations where the underlying base flow is moving, for example, the linear stability studies of Graebel (1964), Georgievskii (1993), Frigaard, Howison & Sobey (1994), Frigaard (2001), Frigaard & Nouar (2003), Peng & Zhu (2004), Landry *et al.* (2006), Métivier, Nouar & Brancher (2005), and the nonlinear stability of Nouar & Frigaard (2001). These all lead to exponential (viscous) decay when stable. The yield stress influences the stability limits and the exponential decay rates, but finite time decay is not found. For the linear stability studies, it is possible to linearize the Navier–Stokes equations in the yielded regions of the base flow, unlike here.

A brief outline of the paper is as follows. In §2, we outline the Rayleigh–Bénard problem for a Bingham fluid, introduce the steady-state solution and stability equations. Our formal analytical results are in §3. We deal with linear stability, global energy stability and conditional stability, in sequence. Section 4 presents computational results. A brief description is given of the methodology and this is followed by results that are illustrative of our analysis. The paper concludes with a section in which we discuss the extensions of our results to different geometries and boundary conditions, the incorporation of residual stresses and how the analysis must be modified for inclined channels.

2. The Rayleigh–Bénard paradigm

We consider here the simplest Rayleigh–Bénard problem with a yield stress fluid, namely that in which a Bingham fluid fills the space between two horizontal plates, the lower of which is heated. Although we specify the problem in three-dimensions, our analysis assumes that the flow instability is two-dimensional. This approach enables analysis (and later computation) to be performed in the most straightforward manner. Later, see §5, we shall discuss three-dimensional perturbations.

Consider a three-dimensional cell, Ω, periodic in (x, y)-directions and bounded in the z-direction by plates at $z = 0$ and $z = 1$. The dimensionless Navier–Stokes and energy equations (assuming the Boussinesq approximation), are:

$$\left.\begin{aligned}
\frac{1}{Pr}\frac{\mathrm{D}u_i}{\mathrm{D}t} &= -\frac{\partial p}{\partial x_i} + \frac{\partial \tau_{ij}}{\partial x_j} + Ra\,\delta_{iz}, \\
\frac{\partial u_i}{\partial x_i} &= 0, \\
\frac{\mathrm{D}T}{\mathrm{D}t} &= \frac{\partial^2 T}{\partial x_j^2},
\end{aligned}\right\} \tag{2.1}$$

for $i, j = 1, 2, 3$, with $(x_1, x_2, x_3) = (x, y, z)$, where $\mathrm{D}/\mathrm{D}t$ denotes the material derivative. A Bingham fluid is the simplest yield stress fluid, with constitutive relationship:

$$\left.\begin{aligned}
\tau_{ij} &= \left(1 + \frac{B}{\dot{\gamma}}\right)\dot{\gamma}_{ij} && \text{iff} \quad \tau > B, \\
\dot{\gamma} &= 0 && \text{iff} \quad \tau \leqslant B,
\end{aligned}\right\} \tag{2.2}$$

where

$$\dot{\gamma} = \sqrt{\tfrac{1}{2}\dot{\gamma}_{ij}\dot{\gamma}_{ij}}, \quad \tau = \sqrt{\tfrac{1}{2}\tau_{ij}\tau_{ij}}.$$

The rate-of-strain tensor $\dot{\gamma}_{ij}$ is defined by:

$$\dot{\gamma}_{ij} = \frac{\partial u_i}{\partial x_j} + \frac{\partial u_j}{\partial x_i}.$$

There are three dimensionless groups governing (2.1). These are:

$$Pr = \frac{\hat{v}}{\hat{\alpha}}, \quad Ra = \frac{\hat{\beta}\hat{g}\Delta\hat{T}\hat{L}^3}{\hat{\alpha}\hat{v}}, \quad B = \frac{\hat{\tau}_Y}{\hat{\rho}\hat{\beta}\hat{g}\Delta\hat{T}\hat{L}}.$$

The Prandtl number, Pr, and Rayleigh number, Ra, are well known. The Bingham number, B, here represents the ratio of yield stress to buoyancy stresses. (Sometimes this is called the Oldroyd number, or yield number. If we were to define a velocity scale by balancing buoyancy and viscous stresses, then B would be the ratio of yield to viscous stresses, which is the usual definition of the Bingham number.) The various dimensional quantities above (denoted with a $\hat{\;}$ symbol), are defined as follows: $\hat{v}$ is the kinematic viscosity (based on the plastic viscosity $\hat{\mu}$), $\hat{\alpha}$ is the thermal diffusivity; $\hat{\beta}$ is the coefficient of thermal expansion, $\hat{g}$ is the acceleration due to gravity, $\Delta\hat{T}$ is the temperature difference between plates, $\hat{L}$ is the vertical separation of the plates, $\hat{\tau}_Y$ is the fluid yield stress, $\hat{\rho}$ is the fluid density.

Boundary conditions at the plates are:

$$u = v = w = 0 \quad \text{at} \quad z = 0, 1, \tag{2.3}$$

$$T = 1 \quad \text{at} \quad z = 0, \quad T = 0 \quad \text{at} \quad z = 1. \tag{2.4}$$

The velocity, pressure and temperature are assumed to be periodic in the (x, y)-directions. Below, we shall suppress the y-direction and consider only two-dimensional perturbations. For these, our periodic cell is assumed to extend over $x \in (0, l)$.

2.1. *Steady-state solution*

The system (2.1)–(2.4) has a steady stratified solution: (U, V, W, P, T) given by

$$U = V = W = 0, \quad P = p_0 - Ra\frac{(1-z)^2}{2}, \quad T = 1 - z. \tag{2.5}$$

This is the basic state of rest of the fluid, in which buoyancy is balanced by hydrostatic pressure, and is the same base state as for the Newtonian fluid ($B = 0$). By virtue of (2.2), even though the velocity is fully determined in the steady state, the shear stress is not, i.e. the shear stress can assume any value below B. We therefore impose:

$$\tau_{ij} = 0. \tag{2.6}$$

In §5.2, we will consider how residual stresses in the static state, may be incorporated into our results.

2.2. *Stability equations*

We assume the steady solution (2.5) is disturbed by a two-dimensional perturbation:

$$(U + u, W + w, P + p, T + \theta).$$

We subtract the x-momentum, z-momentum and energy equations for the steady state, from those for the perturbed state, multiply by (u, w, θ), and integrate over Ω:

$$\Omega = \{(x, z) \in (0, l) \times (0, 1)\}.$$

Under the assumptions of incompressibility, boundary conditions (2.3)–(2.4), and periodicity at $x = 0, l$, we derive the following energy equations:

$$\frac{1}{Pr}\frac{\mathrm{d}H}{\mathrm{d}t} = Ra\langle w\theta \rangle - B\langle \dot{\gamma} \rangle - \langle \dot{\gamma}^2 \rangle, \tag{2.7}$$

$$\frac{\mathrm{d}K}{\mathrm{d}t} = \langle w\theta \rangle - \langle |\nabla\theta|^2 \rangle, \tag{2.8}$$

where

$$\langle f \rangle = \int_{\Omega} f \, \mathrm{d}x, \quad H = \tfrac{1}{2}\langle \boldsymbol{u}^2 \rangle, \quad K = \tfrac{1}{2}\langle \theta^2 \rangle,$$

for $\boldsymbol{u} = (u, w)$. We note that these are the usual energy equations: (2.7) for evolution of the kinetic energy of the perturbation $H(t)$; (2.8) for evolution of the internal energy of the perturbation $K(t)$. The only difference from the Newtonian problem is inclusion of the term $B\langle \dot{\gamma} \rangle$ in (2.7). Energy equations of the same form are found if three-dimensional perturbations are considered.

3. Stability analysis

The remainder of our stability analysis concerns the energy equations (2.7) and (2.8). For a purely viscous (or even visco-elastic) fluid, a classical approach would involve linearizing about the steady state and deriving conditions under which the linearized equations admit stable/unstable eigenmodes. As we have discussed in §1, such an approach does not help here. When the base state is static, the rate of strain of the base state is zero, and hence the effective viscosity is infinite, so that linearization is not possible. If instead we consider a linear perturbation of the stress tensor, for finite B and zero residual stresses, the perturbed stress is also below the yield value. Hence, this also does not lead to a stability problem, but suggests linear stability w.r.t. stress perturbations. Weakly nonlinear theories are extended from the least stable modes of the linear theory, and therefore are of little use for yield stress fluids. This explains our reliance on the energy method, (2.7) and (2.8), i.e. it is the only method left open to us.

3.1. *Linear stability*

We consider first the linear stability of the Rayleigh–Bénard system to two-dimensional disturbances, via energy estimates. Our analysis is summarized in the following result.

THEOREM 1. *Let $E = (1/Pr)H + K$ be the total energy of the Rayleigh–Bénard system. There exist constants C_P and C_{TS} depending only on the dimension and the domain of integration, such that*

$$E(0) < \frac{1}{2}\left(\frac{BC_{TS}}{Ra+1}\right)^2$$

implies:

(i) Exponential decay of the total energy E:

$$E(t) \leqslant E(0)\,\mathrm{e}^{-\alpha t} \quad \text{for } t \geqslant 0.$$

(ii) Finite time decay of $\|\boldsymbol{u}\|$:

$$\|\boldsymbol{u}\|(t) \leqslant \left(\|\boldsymbol{u}\|(0) + \frac{\beta}{\alpha_u}\right)\mathrm{e}^{-\alpha_u t} - \frac{\beta}{\alpha_u} \quad \text{for } 0 \leqslant t \leqslant t_0$$

and

$$\|\boldsymbol{u}\|(t) = 0 \quad \text{for } t \geqslant t_0.$$

(iii) Exponential decay of $\|\theta\|$:

$$\|\theta\|(t) \leqslant \frac{BC_{TS}}{Ra+1}\mathrm{e}^{-\alpha t/2} \quad \text{for } 0 \leqslant t \leqslant t_0$$

and

$$\|\theta\|(t) \leqslant \frac{BC_{TS}}{Ra+1} e^{-\alpha t_0/2 - \tilde{C}_p(t-t_0)}, \quad for \; t \geqslant t_0.$$

Here

$$\alpha = 2\min(PrC_P, \tilde{C}_p), \quad t_0 = \frac{1}{\alpha_u} \ln\left(1 + \frac{\alpha_u}{\beta Pr}\|\boldsymbol{u}\|(0)\right),$$

with

$$\beta = \frac{PrBC_{TS}}{Ra+1}, \quad \alpha_u = PrC_P.$$

Proof. (i) Combining (2.7) and (2.8), we have

$$\frac{\mathrm{d}E}{\mathrm{d}t} = (Ra+1)\langle w\theta \rangle - B\langle \dot{\gamma} \rangle - \langle \dot{\gamma}^2 \rangle - \langle |\nabla\theta|^2 \rangle. \tag{3.1}$$

By the Cauchy–Schwarz inequality,

$$\langle w\theta \rangle \leqslant \|w\|\|\theta\| \leqslant \|\boldsymbol{u}\|\|\theta\|, \tag{3.2}$$

where $\|\cdot\|$ represents the L^2 norm of the corresponding function. On the other hand, the Poincaré inequality and Korn's inequality imply that

$$\tilde{C}_P\langle \theta^2 \rangle \leqslant \langle |\nabla\theta|^2 \rangle, \tag{3.3}$$

$$C_P\langle \boldsymbol{u}^2 \rangle \leqslant \langle |\nabla\boldsymbol{u}|^2 \rangle = \langle \dot{\gamma}^2 \rangle, \tag{3.4}$$

where $\tilde{C}_P$ and C_P are considered to be the optimal constants in the Poincaré inequality, which depend only on the dimension and on the domain of integration.

Owing to the boundary conditions, we note that unless $\boldsymbol{u} = 0$, the velocity $\boldsymbol{u}$ does not represent a rigid-body motion. For such $\boldsymbol{u} \neq 0$, it is shown in Témam & Strang (1980) that there exists a constant C_{TS} such that

$$C_{TS}\|\boldsymbol{u}\| \leqslant \langle \dot{\gamma} \rangle, \tag{3.5}$$

where again C_{TS} depends only on the dimension and the domain of integration. The estimates (3.2)–(3.5) yield

$$\frac{\mathrm{d}E}{\mathrm{d}t} \leqslant (Ra+1)\|\boldsymbol{u}\|\|\theta\| - BC_{TS}\|\boldsymbol{u}\| - C_P\langle \boldsymbol{u}^2 \rangle - \tilde{C}_P\langle \theta^2 \rangle$$

$$\leqslant [(Ra+1)\|\theta\| - BC_{TS}]\|\boldsymbol{u}\| - 2\min(PrC_P, \tilde{C}_P)E,$$

for $t \geqslant 0$. Hence, with $\alpha = 2\min(PrC_P, \tilde{C}_P)$,

$$\frac{\mathrm{d}E}{\mathrm{d}t}(0) < -\alpha E(0) \quad \text{if} \quad \|\theta\|(0) < \frac{BC_{TS}}{Ra+1}.$$

This implies that there exists $\delta > 0$, such that

$$E(t) < E(0) \quad \text{for} \quad 0 < t < \delta$$

and consequently

$$\|\theta\|(t) \leqslant \sqrt{2E(t)} < \sqrt{2E(0)} \quad \text{for} \quad 0 < t < \delta.$$

Therefore, for $0 < t < \delta$,

$$\frac{\mathrm{d}E}{\mathrm{d}t}(t) < -\alpha E(t)$$

whenever

$$E(0) < \frac{1}{2} \left(\frac{BC_{TS}}{Ra+1} \right)^2 . \tag{3.6}$$

By integrating,

$$E(t) \leqslant E(0) \mathrm{e}^{-\alpha t} \quad \text{for } 0 \leqslant t < \delta.$$

By repeating the above argument, starting from $t = \delta/2$, we can keep enlarging the time interval in which the exponential decay of $E(t)$ holds and conclude that

$$E(t) \leqslant E(0) \mathrm{e}^{-\alpha t} \quad \text{for } t \geqslant 0.$$

(ii) We substitute estimates (3.2), (3.4) and (3.5) into (2.7), and further assume that (3.6) holds. If $\|\boldsymbol{u}\| > 0$, for $t \geqslant 0$ we have:

$$\frac{1}{Pr} \frac{\mathrm{d}\|\boldsymbol{u}\|}{\mathrm{d}t} \leqslant (Ra\|\theta\| - BC_{TS}) - C_p\|\boldsymbol{u}\|$$

$$\frac{\mathrm{d}\|\boldsymbol{u}\|}{\mathrm{d}t} \leqslant \left(\frac{Ra}{Ra+1} \mathrm{e}^{-\alpha t/2} - 1 \right) PrBC_{TS} - PrC_p\|\boldsymbol{u}\| \tag{3.7}$$

$$\leqslant -\frac{PrBC_{TS}}{Ra+1} - PrC_p\|\boldsymbol{u}\|. \tag{3.8}$$

If we denote

$$\beta = \frac{PrBC_{TS}}{Ra+1}, \quad \alpha_u = PrC_P,$$

then (3.8) implies, via Gronwall's lemma that:

$$\|\boldsymbol{u}\|(t) \leqslant \left(\|\boldsymbol{u}\|(0) + \frac{\beta}{\alpha_u} \right) \mathrm{e}^{-\alpha_u t} - \frac{\beta}{\alpha_u} \quad \text{for } t \geqslant 0. \tag{3.9}$$

Setting

$$t_0 = \frac{1}{\alpha_u} \ln \left(1 + \frac{\alpha_u}{\beta} \|\boldsymbol{u}\|(0) \right), \tag{3.10}$$

we see that (3.9) yields

$$\|\boldsymbol{u}\|(t) = 0 \quad \text{for } t \geqslant t_0.$$

(iii) From our decay estimate for $E(t)$ in (i), we have directly:

$$\|\theta\|(t) \leqslant \sqrt{2E(t)} \leqslant \frac{BC_{TS}}{Ra+1} \mathrm{e}^{-\alpha t/2} \quad \text{for } t \geqslant 0.$$

However, for $t \geqslant t_0$, we have seen that the velocity is zero. Hence, using estimate (3.4) in (2.8), we have the faster decay estimate:

$$\frac{\mathrm{d}\|\theta\|}{\mathrm{d}t} \leqslant -\tilde{C}_P\|\theta\| \quad \text{for } t \geqslant t_0.$$

We then conclude again by Gronwall's lemma that

$$\|\theta\|(t) \leqslant \|\theta\|(t_0) \mathrm{e}^{-\tilde{C}_P t} \leqslant \frac{BC_{TS}}{Ra+1} \mathrm{e}^{-\alpha t_0/2 - \tilde{C}_P(t-t_0)} \quad \text{for } t \geqslant t_0.$$

Remark 1. Note that linear stability follows from the condition:

$$E(0) < \frac{1}{2} \left(\frac{BC_{TS}}{Ra+1} \right)^2$$

for any finite $B > 0$, i.e. for any finite positive yield stress. To see this, assume that $\|\theta\|(0) = \epsilon$ and $\|\boldsymbol{u}\|(0) = \epsilon K_{\boldsymbol{u}}$, for some arbitrary $O(1)$ constant, $K_{\boldsymbol{u}}$. Then by linear stability we mean that perturbations decay for infinitesimally small $\epsilon \to 0$. Here, we clearly have the result that the flow is stable if:

$$\epsilon < \frac{BC_{TS}}{Ra + 1}\left(\frac{K_{\boldsymbol{u}}}{Pr} + 1\right)^{-1/2}, \tag{3.11}$$

i.e. we also have stability for small finite ϵ, or weak conditional stability. Viewed another way, for given ϵ there is a stability bound on B, of form $B \geqslant O(\epsilon Ra)$.

The result is therefore clearly much stronger than that given by the usual linear stability analysis. In addition to decay, we have the decay of the velocity perturbation in a finite time, i.e. this is more than asymptotically stable. We may summarize the results in the following statements:

(*a*) For any finite strictly positive B (yield stress), the steady state is linearly asymptotically stable for all Ra and Pr.

(*b*) A sufficiently small finite perturbation, satisfying (3.11), is asymptotically stable.

(*c*) In both cases, stability is characterized by decay of the velocity to zero within a finite time t_0. The temperature decay is exponential, but the rate increases after convection has switched off at $t = t_0$.

Remark 2. The finite time decay time scale in (3.10) is simplest to state, but is conservative. If $\alpha_{\boldsymbol{u}} > \alpha/2$, then we have for $t \geqslant 0$

$$\|\boldsymbol{u}\|(t) \leqslant \left(\|\boldsymbol{u}\|(0) + \frac{\tilde{\beta}}{\alpha_{\boldsymbol{u}}} - \frac{\tilde{\beta} Ra}{(\alpha_{\boldsymbol{u}} - \alpha/2)(Ra + 1)}\right)e^{-\alpha_{\boldsymbol{u}} t} + \frac{\tilde{\beta} Ra\, e^{-\alpha t/2}}{(\alpha_{\boldsymbol{u}} - \alpha/2)(Ra + 1)} - \frac{\tilde{\beta}}{\alpha_{\boldsymbol{u}}}, \tag{3.12}$$

which decays to zero at $t < t_0$; here, $\tilde{\beta} = Pr B C_{TS}$. On the other hand, if $\alpha_{\boldsymbol{u}} = \alpha/2$, then the estimate

$$\|\boldsymbol{u}\|(t) \leqslant \left(\|\boldsymbol{u}\|(0) + \frac{\tilde{\beta}}{\alpha_{\boldsymbol{u}}} + \frac{\tilde{\beta} Ra}{Ra + 1}t\right)e^{-\alpha_{\boldsymbol{u}} t} - \frac{\tilde{\beta}}{\alpha_{\boldsymbol{u}}}, \tag{3.13}$$

holds for $t \geqslant 0$. Again the decay to zero is at a time $t < t_0$.

Focusing on (3.10), we see that t_0 decreases if B increases, or Pr increases, or Ra decreases, or if $\|\boldsymbol{u}\|(0)$ decreases, all of which effects are physically intuitive.

3.2. *Nonlinear stability*

From the results of Theorem 1, we are led to question two things. First, we have seen that the linear stability results certainly extend to small finite perturbations. Therefore, we ask whether the finite limit of the perturbation is optimal in Theorem 1, or whether it can be improved in some way. For example, for Newtonian fluids, it is known that the flow is globally asymptotically stable for $Ra < Ra_E$, where Ra_E depends upon the domain and boundary conditions imposed. Secondly, we have observed that decay of the velocity to zero occurs over a finite time scale, whereas for a Newtonian fluid, the decay time scale is infinite (exponential decay). We therefore also question whether finite time decay of the velocity holds true for all (Ra, Pr, B) and all initial conditions for which there is some form of stability? These are the goals of this section. First, we review the known results for Newtonian fluids.

3.2.1. *Summary of Newtonian results*

A good overview of the key results for the Rayleigh–Bénard problem for a Newtonian fluid may be found in Koschmieder (1993). The energy stability of the

Rayleigh–Bénard system is reviewed by Joseph (1976), which also covers the earlier results of Ukhovskii & Iudovich (1963), Sani (1964), Joseph (1965) and Joseph (1966). From these, it is known that there exists a critical Rayleigh number $Ra_E > 0$ such that:

$$\frac{\mathrm{d}E}{\mathrm{d}t} = \begin{cases} < 0 & \text{if } Ra < Ra_E, \\ 0 & \text{if } Ra = Ra_E, \end{cases}$$

where the energy $E(t)$ is defined as

$$E(t) = \frac{1}{Pr}H(t) + Ra_E K(t).$$

For the Newtonian results, the energy limit, $Ra = Ra_E$, is identical with the linear stability limit, Ra_L. This is because (i) the base state has zero velocity; (ii) linear marginal stability for the Rayleigh–Bénard problem involves the exchange of stabilities. Under these conditions, the eigenfunction that satisfies the linear stability equations at marginal stability also satisfies the variational equations of the energy stability problem. Hence, $Ra_E = Ra_L$. In fact, there are a range of hydrodynamic stability problems that share this characteristic (Joseph 1976). The critical Rayleigh number limit for the Newtonian fluid with (rigid–rigid) Dirichlet conditions at $z = 0$, l, is $Ra_E = Ra_L = 1707.8$ (see Koschmieder 1993). For rigid–free and free–free boundary conditions, the linear limits are $Ra_L = 1100.7$ and $Ra_L = 657.5$, respectively.

We assume below that the sets of admissible functions for the Newtonian and Bingham fluid problems are the same, and denote this set by S. (For the Bingham problem we would expect that each of u, w, θ are in closed subsets of $H^1(\Omega)$, defined by the specific boundary and periodicity conditions, and further restricted by the divergence-free constraint in the case of the velocity components. The variational results for the Newtonian fluid, which we shall make comparison with, do not rely on further regularity than $H^1(\Omega)$. The boundary and periodicity conditions are identical for Newtonian and Bingham problems.) First, let us consider energy stability for the Newtonian fluid, setting $B = 0$ in (2.7)–(2.8). For $\nu > 0$, consider the energy $E_\nu(t)$ defined by:

$$E_\nu(t) = \frac{H(t)}{Pr} + \nu K(t).$$

On summing (2.7) and (2.8), we see that $E_\nu(t)$ satisfies the following differential inequality.

$$\frac{\mathrm{d}}{\mathrm{d}t}E_\nu \leqslant -[\langle \dot{\gamma}^2 \rangle + \nu\langle |\nabla\theta|^2 \rangle]\left[1 - (Ra + \nu)\sup_{(\tilde{u},\tilde{\theta})\in S}\left\{\frac{\langle \tilde{w}\tilde{\theta} \rangle}{\langle \tilde{\dot{\gamma}}^2 \rangle + \nu\langle |\nabla\tilde{\theta}|^2 \rangle}\right\}\right]. \qquad (3.14)$$

We define $G(\nu)$ by:

$$\frac{1}{G(\nu)} = \sup_{(\tilde{u},\tilde{\theta})\in S}\left\{\frac{\langle \tilde{w}\tilde{\theta} \rangle}{\langle \tilde{\dot{\gamma}}^2 \rangle + \nu\langle |\nabla\tilde{\theta}|^2 \rangle}\right\}$$

and note that by rescaling $\tilde{\theta}$, for any ν_1, ν_2 we have:

$$\frac{\sqrt{\nu_1}}{G(\nu_1)} = \frac{\sqrt{\nu_2}}{G(\nu_2)}.$$

Furthermore, setting $\nu = Ra_E$ and $Ra = Ra_E$ in (3.14) produces the energy limit for Newtonian flow, i.e.

$$2Ra_E = G(Ra_E) \Rightarrow G(\nu) = 2\sqrt{\nu Ra_E}.$$

Therefore, $E_\nu(t)$ satisfies:

$$\frac{\mathrm{d}}{\mathrm{d}t} E_\nu \leqslant -2 \min(Pr C_P, \tilde{C}_P) \left[1 - \frac{Ra + \nu}{2\sqrt{\nu Ra_E}} \right] E_\nu(t) \quad \text{if } Ra + \nu < 2\sqrt{\nu Ra_E}. \quad (3.15)$$

The minimum ratio $(Ra + \nu)/\sqrt{\nu}$ is found when $\nu = Ra$ and energy stability is thus first achieved for $\nu = Ra < Ra_E$. The energy functional $E(t)$ that we consider is for $\nu = Ra_E$, for which we have

$$\frac{\mathrm{d}}{\mathrm{d}t} E \leqslant -\min(Pr C_P, \tilde{C}_P) \left[1 - \frac{Ra}{Ra_E} \right] E(t) \quad \text{if } Ra < Ra_E \quad (3.16)$$

3.2.2. *Global asymptotic stability and finite time decay of* $\|u\|(t)$ *for* $Ra < Ra_E$

The energy equations (2.7)–(2.8) for the perturbation may be rewritten as follows:

$$\frac{1}{Pr} \frac{\mathrm{d}H}{\mathrm{d}t} = Ra \langle w\theta \rangle - B \langle \dot{\gamma} \rangle - \langle \dot{\gamma}^2 \rangle, \quad (3.17a)$$

$$Ra_E \frac{\mathrm{d}K}{\mathrm{d}t} = Ra_E \langle w\theta \rangle - Ra_E \langle |\nabla\theta|^2 \rangle. \quad (3.17b)$$

We may note from (3.16) and (3.17) that, if $Ra < Ra_E$, then the energy $E(t)$ of the Bingham fluid flow ($B > 0$) also decays, since the energy stability analysis may proceed by neglecting the Bingham term in (3.17). Thus, we may infer that the Bingham fluid flow is at least as stable as the corresponding Newtonian fluid flow. The following theorem, however, gives a more precise statement.

THEOREM 2. *Let* $E = (1/Pr)H + Ra_E K$ *be the total energy of the Rayleigh–Bénard system. There exist constants* C_P *and* C_{TS} *depending only on the dimension and the domain of integration, such that* $Ra < Ra_E$ *implies:*

(i) Exponential decay of the total energy E:

$$E(t) \leqslant E(0)\,\mathrm{e}^{-\alpha t} \quad \text{for } t \geqslant 0.$$

(ii) Finite time decay of $\|u\|$:

$$\|u\|(t) \leqslant \left(\|u\|(0) + \frac{\beta_2}{\alpha_u} - \frac{\beta_1}{\alpha_u - \alpha/2} \right) \mathrm{e}^{-\alpha_u t} + \frac{\beta_1}{\alpha_u - \alpha/2}\, \mathrm{e}^{-\alpha t/2} - \frac{\beta_2}{\alpha_u}$$

for $0 \leqslant t \leqslant t_0$ *and*

$$\|u\|(t) = 0 \quad \text{for } t \geqslant t_0.$$

(iii) Exponential decay of $\|\theta\|$:

$$\|\theta\|(t) \leqslant \sqrt{\frac{2E(0)}{Ra_E}}\, \mathrm{e}^{-\alpha t/2} \quad \text{for } 0 \leqslant t \leqslant t_0$$

and

$$\|\theta\|(t) \leqslant \sqrt{\frac{2E(0)}{Ra_E}}\, \mathrm{e}^{-\alpha t_0/2 - \tilde{C}_P(t - t_0)} \quad \text{for } t \geqslant t_0,$$

where

$$\alpha = \min(Pr C_P, \tilde{C}_P) \left(1 - \frac{Ra}{Ra_E} \right), \quad \alpha_u = Pr C_P,$$

$$\beta_1 = Pr Ra \sqrt{\frac{2E(0)}{Ra_E}}, \quad \beta_2 = Pr B C_{TS}$$

and t_0 is the root of

$$\left(\|\boldsymbol{u}\|(0) + \frac{\beta_2}{\alpha_u} - \frac{\beta_1}{\alpha_u - \alpha/2} \right) \mathrm{e}^{-\alpha_u t} + \frac{\beta_1}{\alpha_u - \alpha/2} \mathrm{e}^{-\alpha t/2} - \frac{\beta_2}{\alpha_u} = 0.$$

Proof

(i) Assume that $Ra < Ra_E$ and that $E(t) > 0$. Neglecting the yield stress dissipation, we have

$$\frac{\mathrm{d}E}{\mathrm{d}t} = (Ra + Ra_E)\langle w\theta \rangle - B\langle \dot{\gamma} \rangle - \langle \dot{\gamma}^2 \rangle - Ra_E \langle |\nabla\theta|^2 \rangle$$

$$\leqslant - \left[\langle \dot{\gamma}^2 \rangle + Ra_E \langle |\nabla\theta|^2 \rangle \right] \left[1 - (Ra + Ra_E) \sup_{(\tilde{\boldsymbol{u}}, \tilde{\theta}) \in S} \left\{ \frac{\langle \tilde{w}\tilde{\theta} \rangle}{\langle \tilde{\gamma}^2 \rangle + Ra_E \langle |\nabla\tilde{\theta}|^2 \rangle} \right\} \right].$$

Then, following the Newtonian analysis leading to (3.16), we have

$$\frac{\mathrm{d}E}{\mathrm{d}t} \leqslant - \min(PrC_P, \tilde{C}_P) \left(1 - \frac{Ra}{Ra_E} \right) E,$$

for $t \geqslant 0$. Therefore, with $\alpha = \min(PrC_P, \tilde{C}_P) \left(1 - \frac{Ra}{Ra_E} \right)$,

$$E(t) \leqslant E(0)\, \mathrm{e}^{-\alpha t} \quad \text{for } t \geqslant 0. \tag{3.18}$$

(ii) From (3.18), we see that

$$\|\theta\|(t) \leqslant \sqrt{\frac{2E(t)}{Ra_E}} \leqslant \sqrt{\frac{2E(0)}{Ra_E}}\, \mathrm{e}^{-\alpha t/2} \quad \text{for } t \geqslant 0. \tag{3.19}$$

We assume $\|\boldsymbol{u}\| > 0$, and substitute the above bound, with (3.2) and (3.4), into (3.17a):

$$\frac{\mathrm{d}\|\boldsymbol{u}\|}{\mathrm{d}t} \leqslant Pr \left(Ra\sqrt{\frac{2E(0)}{Ra_E}}\, \mathrm{e}^{-\alpha t/2} - BC_{TS} \right) - PrC_p\|\boldsymbol{u}\| \quad \text{for } t \geqslant 0. \tag{3.20}$$

Denote

$$\beta_1 = PrRa\sqrt{\frac{2E(0)}{Ra_E}}, \quad \beta_2 = PrBC_{TS}, \quad \alpha_u = PrC_P.$$

Then (3.20) combined with Gronwall's lemma gives, for $t \geqslant 0$.:

$$\|\boldsymbol{u}\|(t) \leqslant \left(\|\boldsymbol{u}\|(0) + \frac{\beta_2}{\alpha_u} - \frac{\beta_1}{\alpha_u - \alpha/2} \right) \mathrm{e}^{-\alpha_u t} + \frac{\beta_1}{\alpha_u - \alpha/2} \mathrm{e}^{-\alpha t/2} - \frac{\beta_2}{\alpha_u}, \tag{3.21}$$

It is evident that the first two terms above decay until dominated by the last term. Therefore, let t_0 be the root of

$$\left(\|\boldsymbol{u}\|(0) + \frac{\beta_2}{\alpha_u} - \frac{\beta_1}{\alpha_u - \alpha/2} \right) \mathrm{e}^{-\alpha_u t} + \frac{\beta_1}{\alpha_u - \alpha/2} \mathrm{e}^{-\alpha t/2} - \frac{\beta_2}{\alpha_u} = 0.$$

Then (3.21) yields

$$\|\boldsymbol{u}\|(t) = 0 \quad \text{for } t \geqslant t_0.$$

(iii) For all $t \geqslant 0$, the decay estimate (3.19) holds. From (2.8), when $t \geqslant t_0$, we have the faster decay:

$$\frac{\mathrm{d}\|\theta\|}{\mathrm{d}t} \leqslant -\tilde{C}_P\|\theta\|.$$

In this range:

$$\|\theta\|(t) \leqslant \|\theta\|(t_0)\exp(-\tilde{C}_P t) \leqslant \sqrt{\frac{2E(0)}{Ra_E}}\exp(-\alpha t_0/2 - \tilde{C}_P(t - t_0)).$$

Remark 3. Thus, for $Ra \leqslant Ra_E$, the Bingham fluid flow is also asymptotically globally stable. Furthermore, the characteristic decay of the velocity in a finite time is also found. The conditional bounds of Theorem 1 are therefore clearly not optimal for this range of Ra. On the other hand, since $Ra_E = Ra_L$ for the Newtonian fluid, whereas theorem 1 gives linear stability also for $Ra > Ra_L$, we see that in terms of stability conditions on Ra, Theorem 2 is also not optimal. We therefore consider how the conditional bounds may be extended to $Ra > Ra_E$.

3.2.3. *Conditional stability for $Ra > Ra_E$*

Considering (2.7) and (2.8), we observe that for a sufficiently large initial perturbation, the term $B\langle\dot{\gamma}\rangle$ scales only linearly with the perturbation, whereas all other terms are quadratic in the perturbation. Thus, it seems likely that the Newtonian limit Ra_E is also the global stability limit of the Bingham fluid flow, i.e. for sufficiently large initial perturbation the yield stress term is insignificant. Therefore, for $Ra > Ra_E$, we expect to only find stability of the system (2.7) and (2.8), conditional on the size of the initial perturbations $\|\boldsymbol{u}\|(0)$ and $\|\theta\|(0)$. Here, we consider an energy functional $E(t)$ defined by:

$$E(t) = \frac{1}{Pr}H(t) + RaK(t).$$

From (2.7), (2.8), we have

$$\frac{\mathrm{d}E}{\mathrm{d}t} = 2Ra_E\langle w\theta\rangle - \langle\dot{\gamma}^2\rangle - Ra_E\langle|\nabla\theta|^2\rangle + (Ra - Ra_E)[2\langle w\theta\rangle - \langle|\nabla\theta|^2\rangle] - B\langle\dot{\gamma}\rangle,$$

$$\leqslant (Ra - Ra_E)\left(2\|\boldsymbol{u}\|\|\theta\| - \tilde{C}_P\|\theta\|^2\right) - BC_{TS}\|\boldsymbol{u}\|. \quad (3.22)$$

We define $F(\|\boldsymbol{u}\|, \|\theta\|)$ by

$$F(\|\boldsymbol{u}\|, \|\theta\|) = (Ra - Ra_E)\left(2\|\boldsymbol{u}\|\|\theta\| - \tilde{C}_P\|\theta\|^2\right) - BC_{TS}\|\boldsymbol{u}\|,$$

which is a smooth function in the first quadrant of the $(\|\boldsymbol{u}\|, \|\theta\|)$-plane. Under the assumption that $Ra > Ra_E$, the stability of the system can be expected if the initial perturbation $(\|\boldsymbol{u}\|(0), \|\theta\|(0))$ is chosen to ensure both $F(\|\boldsymbol{u}\|(0), \|\theta\|(0)) < 0$ and $F(\|\boldsymbol{u}\|(t), \|\theta\|(t)) < 0$ for all $t > 0$. Geometrically, the condition that $F(\|\boldsymbol{u}\|(t), \|\theta\|(t)) < 0$ for all $t > 0$, implies that the phase paths of $(\|\boldsymbol{u}\|, \|\theta\|)$ cross the level sets $E = $ constant, inwards only. Consequently, for stability we require that $E(0) < E^*$, where

$$\frac{1}{Pr}\|\boldsymbol{u}\|^2 + Ra\|\theta\|^2 = E^*,$$

is the largest quarter ellipse in the first quadrant of the $(\|\boldsymbol{u}\|, \|\theta\|)$-plane, that touches the curve $F(\|\boldsymbol{u}\|, \|\theta\|) = 0$. The definition of E^* is illustrated in figure 1(*a*) for parameters $Ra = 1750$, $Ra_E = 1707.8$, $B = 10$, $Pr = 1$, $\tilde{C}_P = \pi^2$, $C_{TS} = 1$. In general, E^* decays with Ra and Pr, but increases with B, as illustrated in figure 1(*c*, *d*). It remains to consider the decay rate of the perturbation. We have the following result.

THEOREM 3. *Let $E(t) = H(t)/Pr + RaK(t)$ be the total energy of the Rayleigh–Bénard system. There exists a constant E^*, depending only on the domain Ω and on Ra, Pr and B, such that $E(0) < E^*$ implies*

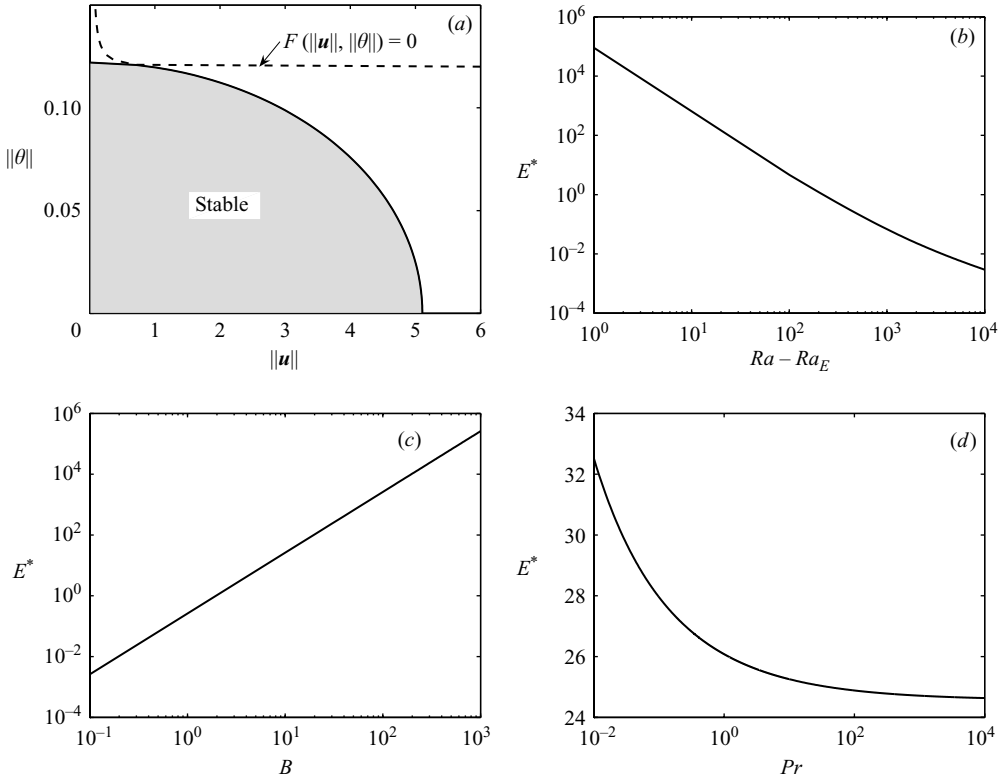FIGURE 1. (a) Illustration of the definition of E^*, for parameters $Ra = 1750$, $Ra_E = 1707.8$, $B = 10$, $Pr = 1$, $\tilde{C}_P = \pi^2$, $C_{TS} = 1$; (b) variation of E^* with $Ra > Ra_E$, other parameters as in (a); (c) variation of E^* with B, other parameters as in (a); (d) variation of E^* with Pr, other parameters as in (a).

(i) *Decay of the total energy* E:

$$E(t) < E(0) \quad for \ t > 0,$$

with exponential decay of E, for $t > t_0 + t_1$, defined below.

(ii) *Finite time decay of* $\|\boldsymbol{u}\|$. *There exist constants* C^* *and* q, *such that*:
If $E^* > C^*$, then

$$\|\boldsymbol{u}\|(t) \leqslant \left(\|\boldsymbol{u}\|(0) + \frac{BC_{TS}}{2C_P} \right) \exp(-PrC_P t) - \frac{BC_{TS}}{2C_P} \quad for \ 0 \leqslant t \leqslant t_0,$$

$$\|\boldsymbol{u}\|(t) = 0 \quad for \ t \geqslant t_0.$$

If $E^* \leqslant C^*$, then

$$\|\boldsymbol{u}\|(t) \leqslant \left(\|\boldsymbol{u}\|(t_1) + \frac{BC_{TS}}{2C_P} \right) \exp(-PrC_P t) - \frac{BC_{TS}}{2C_P} \quad for \ t_1 \leqslant t \leqslant t_0 + t_1$$

$$\|\boldsymbol{u}\|(t) = 0, \quad for \ t \geqslant t_0 + t_1.$$

(iii) *Exponential decay of* $\|\theta\|$:
If $E^* > C^*$, then

$$\|\theta\|(t) \leqslant \|\theta\|(t_0) \exp(-\tilde{C}_P(t - t_0)) \quad for \ t \geqslant t_0.$$

If $E^* \leqslant C^*$, then

$$\|\theta\|(t) \leqslant \|\theta\|(t_0 + t_1) \exp(-\tilde{C}_P(t - t_0 - t_1)) \quad \text{for } t \geqslant t_0 + t_1,$$

Here

$$t_0 = \frac{1}{PrC_P} \ln\left(1 + \frac{2C_P\|\boldsymbol{u}\|(0)}{BC_{TS}}\right), \quad t_1 = \frac{E(0) - C^*}{q}.$$

Proof. (i) We note that E^* depends only on Ω and on Ra, Pr, B. If $E(0) < E^*$, then $F(\|\boldsymbol{u}\|(0), \|\theta\|(0)) < 0$. There exists $\delta_1 > 0$, such that $E(t) < E(0)$ for all $0 < t < \delta_1$. Since $E(\delta_1/2) < E^*$, starting from $t = \delta_1/2$, there exists $\delta_2 > 0$, such that $E(t) < E(0)$ for all $0 < t < \delta_1/2 + \delta_2$. Repeating this procedure, we conclude that $E(t) < E(0)$ for $t > 0$. We use only the boundedness of $E(t)$ below. Note that exponential decay of $E(t)$ will then follow from the decay implicit in parts (i) and (iii) of the theorem.

(ii) and (iii) We define C^* by:

$$C^* = \frac{B^2 C_{TS}^2}{8Ra}.$$

If $F(\|\boldsymbol{u}\|(0), \|\theta\|(0)) < 0$ and $E(0) < C^*$, then $E(t) < C^*$ and on bounding $\|\theta\|$ by $\sqrt{2E(t)/Ra}$, (2.7) becomes:

$$\frac{\mathrm{d}\|\boldsymbol{u}\|}{\mathrm{d}t} \leqslant Pr\left(Ra\|\theta\| - BC_{TS}\right) - PrC_p\|\boldsymbol{u}\|$$

$$\leqslant -\frac{PrBC_{TS}}{2} - PrC_p\|\boldsymbol{u}\| \qquad \text{for } t > 0.$$

That is,

$$\|\boldsymbol{u}\|(t) \leqslant \left(\|\boldsymbol{u}\|(0) + \frac{BC_{TS}}{2C_P}\right) \exp(-PrC_Pt) - \frac{BC_{TS}}{2C_P} \quad \text{for } 0 \leqslant t \leqslant t_0$$

and

$$\|\boldsymbol{u}\|(t) = 0 \quad \text{for } t \geqslant t_0,$$

where

$$t_0 = \frac{1}{PrC_P} \ln\left(1 + \frac{2C_P\|\boldsymbol{u}\|(0)}{BC_{TS}}\right).$$

As before, for $t \geqslant t_0$, we have pure exponential decay of the temperature, from (2.8).

$$\|\theta\|(t) \leqslant \|\theta\|(t_0) \exp(-\tilde{C}_P(t - t_0)) \quad \text{for } t \geqslant t_0.$$

We next show that even if $E^* > C^*$, we can still expect finite decay of $\|\boldsymbol{u}\|$ and exponential decay of $\|\theta\|$. We start from an arbitrary point $(\|\boldsymbol{u}\|(0), \|\theta\|(0))$ satisfying $K \leqslant E(0) < E^*$. Then $E(t) < E(0) < E^*$ owing to the boundedness of $E(t)$, in (i) above. Let

$$S = \{(\|\boldsymbol{u}\|, \|\theta\|) \mid C^* \leqslant E \leqslant E(0)\}.$$

Then S is a closed bounded subset on the $(\|\boldsymbol{u}\|, \|\theta\|)$-plane, and we may define q:

$$-q = \max_{(\|\boldsymbol{u}\|, \|\theta\|) \in S} F(\|\boldsymbol{u}\|, \|\theta\|).$$

Estimate (3.22) implies that

$$\frac{\mathrm{d}E}{\mathrm{d}t} \leqslant F(\|\boldsymbol{u}\|, \|\theta\|) \leqslant -q \quad \text{for } t > 0.$$

Hence,

$$E(t) \leqslant E(0) - qt \quad \text{for } t > 0$$

and

$$E(t) < C^* \quad \text{for } t > t_1 = \frac{E(0) - C^*}{q}.$$

Combining the decay result from the case $E^* < C^*$ (ii), we conclude that

$$\|\boldsymbol{u}\|(t) \leqslant \left(\|\boldsymbol{u}\|(t_1) + \frac{BC_{TS}}{2C_P}\right) \exp(-PrC_P t) - \frac{BC_{TS}}{2C_P} \quad \text{for } t_1 \leqslant t \leqslant t_0$$

and

$$\|\boldsymbol{u}\|(t) = 0 \quad \text{for } t \geqslant t_0 + t_1,$$

where now

$$t_0 = \frac{1}{PrC_P} \ln\left(1 + \frac{2C_P\|\boldsymbol{u}\|(t_1)}{BC_{TS}}\right).$$

Again for the temperature, once the velocity has decayed to zero, we have:

$$\|\theta\|(t) \leqslant \|\theta\|(t_0 + t_1) \exp(-\tilde{C}_P(t - t_0 - t_1)) \quad \text{for } t \geqslant t_0 + t_1.$$

Remark 4. Thus, under the conditions of Theorem 3, we have again finite time decay of the velocity and (eventually) exponential decay of the temperature. As the boundary $E(0) = E^*$ is approached, the decay time scales become infinite.

3.3. *Summary of analytical results*

To summarize our results, below the energy limit of the analogous Newtonian problem, the Bingham problem is also asymptotically stable to all perturbations. Above the energy stability limit, the Bingham problem is conditionally asymptotically stable to perturbations of sufficiently small initial conditions. As $Ra \to \infty$, the conditional bounds approach zero, and as $Ra \to Ra_E$, the conditional bounds become infinite. Whenever the Bingham problem is asymptotically stable, we have found that the velocity perturbation decays to zero in a finite time. The temperature perturbation decays to zero exponentially, but at a faster rate once there is no convection.

The decay rates and stability bounds are governed by the constants $\tilde{C}_P, C_P, C_{TS}$. For parallel plates with rigid–rigid boundary conditions, π^2 is the best possible for $\tilde{C}_P$. For C_P the value is higher owing to the divergence, free constraint; Joseph (1965) gives $C_P = 3.74\pi^2$. We have not found a value for C_{TS} in the literature. However, the exact value of C_{TS} is not important since the aim here is to describe the qualitative behaviour of the perturbation, rather than compute the exact stopping times or decay rates from our bounds (we expect these to be conservative).

4. Computational solution and results

We have also computed the numerical solution of the system (2.1) and (2.2), with boundary conditions (2.3) and (2.4) in a periodic domain. Computational solution of an initial boundary-value problem is not always an effective way of determining exact stability limits but, as explained in § 1, the usual tools of hydrodynamic stability are not all available to us and direct computation is one of the few methods we can use.

A key dynamical feature of yield stress fluids is that they may come to rest in a finite time, and we have seen this feature predicted in all our analytical results. The simplest computational methods for these flows involve regularization of the effective viscosity

and such methods are often implemented in standard commercial CFD software. However, they are ineffective at predicting stopping behaviour since sub-yield stress flow behaviour is regularized by modelling as a highly viscous fluid. In order to capture the finite time decay, it is necessary to use a more complex method that properly resolves the yielding behaviour of the fluid. Finite time decay is preserved in algorithms that are based on the augmented Lagrangian method, provided close attention is paid to the time-stepping. The computations presented below have been performed using the finite element code CROCO, based on the software component library PELICANS, both developed at IRSN.

4.1. *Outline of computational method*

In short, the numerical strategy used to solve the system (2.1–2.2) follows closely that proposed in Vola, Boscardin & Latché (2003). The methodology outlined in Vola *et al.* (2003) has been developed so as to give a robust numerical scheme, able to cope with a wide range of constitutive laws, without any regularization of the viscosity. Material derivatives in both the momentum and energy equations are discretized by a method of characteristics according to the splitting scheme outlined in §2 and §3.2 of Vola *et al.* (2003). For Newtonian fluids, when coupled to a Galerkin discretization, this method leads to accurate and stable schemes under assumptions that are weaker than the usual CFL conditions.

At each time step (size Δt), we must solve a Helmoltz problem (energy equation) and a generalized Stokes problem (momentum and mass equations). For the sake of readability, subscripts and superscripts referring to time discretization are omitted. An integral formulation of the constitutive law (2.2) is defined using a thermodynamical pseudo-potential $\psi(\dot{\gamma})$:

$$\boldsymbol{\tau} \in \partial_{\dot{\gamma}} \psi(\dot{\gamma}),$$

where $\partial_{\dot{\gamma}} \psi$ denotes the sub-differential of ψ with respect to $\dot{\boldsymbol{\gamma}}$. (See Ekeland & Témam (1976), chapt. 1, §5) for a discussion of sub-differentiability. Most of the commonly used generalized Newtonian fluid models, including those with a yield stress, can be characterized in this way. Loosely speaking, sub-differentiability is a weaker form of differentiability and this is required for yield stress fluids since $\dot{\gamma}$ is not everywhere differentiable). This is characterized as follows:

$$\boldsymbol{\tau} \in \partial_{\dot{\gamma}} \psi(\dot{\gamma}) \quad \Leftrightarrow \quad \forall \boldsymbol{\zeta} \ \psi(\boldsymbol{\zeta}) - \psi(\dot{\boldsymbol{\gamma}}) \geqslant \boldsymbol{\tau} : (\boldsymbol{\zeta} - \dot{\boldsymbol{\gamma}}),$$

where $\boldsymbol{\zeta} : \boldsymbol{\zeta} = \sum_{i,j} \boldsymbol{\zeta}_{ij}^2$. For the Bingham model, this pseudo-potential has the following form:

$$\psi(\dot{\gamma}) = \tfrac{1}{2} \dot{\gamma}^2 + B \dot{\gamma}.$$

Using this characterization, the weak formulation of the momentum equations turns into a variational inequality that is equivalent to the following minimization problem, find $\boldsymbol{u} \in \{\boldsymbol{v} | \nabla \cdot \boldsymbol{v} = 0\}$ such that:

$$\mathscr{G}(\boldsymbol{u}) + \mathscr{F}(\dot{\boldsymbol{\gamma}}(\boldsymbol{u})) = \min_{\boldsymbol{v} | \nabla \cdot \boldsymbol{v} = 0} [\mathscr{G}(\boldsymbol{v}) + \mathscr{F}(\dot{\boldsymbol{\gamma}}(\boldsymbol{v}))], \tag{4.1}$$

where

$$\mathscr{G}(\boldsymbol{v}) = \frac{1}{2\Delta t \, Pr} \int_{\Omega} \boldsymbol{v} \cdot \boldsymbol{v} \, \mathrm{d}x - \int_{\Omega} \left(Ra T \delta_{iz} + \frac{1}{\Delta t \, Pr} \boldsymbol{v}^* \right) \cdot \boldsymbol{v} \, \mathrm{d}x, \tag{4.2}$$

$$\mathscr{F}(\dot{\gamma}(\boldsymbol{v})) = \int_{\Omega} \psi(\dot{\gamma}(\boldsymbol{v})) \, \mathrm{d}x, \tag{4.3}$$

and where $\boldsymbol{v}^*$ denotes the convective velocity found by the method of characteristics.

We follow the decomposition–coordination method of Fortin & Glowinski (1982). First, we introduce an auxiliary primal variable representing the rate of strain tensor $\dot{\boldsymbol{\gamma}}$ together with an associated constraint that ensures that the meaning of (4.1) remains unchanged. This constraint and the incompressibility condition are then relaxed by an augmented Lagrangian technique. The two Lagrangian multipliers are homogeneous to the shear stress and pressure, respectively. The minimization problem (4.1) turns into a four field saddle-point problem. The saddle-point problem is solved with a fully decoupled variant of an algorithm of Uzawa type proposed in Fortin & Glowinski (1982).

The choice of the approximation spaces (piecewise linear velocity and pressure, piecewise constant auxiliary variables and corresponding multipliers, all on triangles), is guided by various requirements described in Latché & Vola (2004). The non-differentiality due to the constitutive law is now isolated in the step of the algorithm associated with the optimality of the primal auxiliary variable representing $\dot{\boldsymbol{\gamma}}$. Moreover, thanks to the choice of the approximation spaces, this step turns into a series of scalar minimization problems (variable $\dot{\gamma}$) that can be solved on each element, and analytically in the case of a Bingham fluid.

The semi-infinite theoretical domain is represented by a two-dimensional computational domain of unit height, and length $l = 2\pi/k_x$. Periodic boundary conditions for all unknown fields are imposed on the vertical boundaries. Thus, choice of k_x, hence the periodicity, is an additional (numerical) parameter that is not present in our analysis. Since our purpose is mostly to illustrate the previous theoretical results, we have fixed $k_x = 3$ for all numerical results presented below, unless otherwise stated. Additionally, we have set $Pr = 1$ throughout. Lastly, it is necessary to prescribe an initial condition, and here we have used:

$$u = w = 0, \quad p = 0 \text{ and } \theta = z(1-z)(0.8 + 0.2 \sin(x^2)) \quad \text{at } t = 0. \tag{4.4}$$

for all computations. Time step and mesh convergence studies have been performed. For the results following, the meshes consist of 1250 triangles and a time step of $\Delta t = 5 \times 10^{-3}$ has been used.

4.2. Sub-critical Rayleigh number: $Ra = 1500$

Here we have $Ra < Ra_E = 1707.8$, and therefore expect decay of all perturbations in the L^2 norm. According to Theorem 2, stability is global, i.e. independent of the size of the initial condition. Secondly, for any non-zero B the velocity should decay to zero in a finite time and the temperature should decay exponentially. Figure 2 shows the computed evolution of $\|\boldsymbol{u}\|$ and $\|\theta\|$, starting from the initial perturbation (4.4). Results are shown for a Newtonian fluids and for two (quite small) Bingham numbers, $B = 0.01$ and $B = 0.1$. We observe that the decay of the Bingham fluid perturbations is qualitatively different to that of the Newtonian fluid. There is an initial viscous decay away from the initial condition. For the smaller B, the Newtonian curve is initially followed very closely. At longer times, the yield stress term dominates and we see the rapid finite time decay of $\|\boldsymbol{u}\|$. We can also discern two distinct decay rates for $\|\theta\|$, with faster decay after $\|\boldsymbol{u}\| = 0$

Apart from the decay rate observed, the way the fluid returns to its steady stratified base state is different for the Bingham fluid. We know that the Newtonian stability problem, even at $Ra = Ra_E$ is characterized by a linear eigenmode. It is therefore perhaps not surprising to observe that for the Newtonian fluid, the distribution of the velocity is relatively unchanged as $\|\boldsymbol{u}\| \to 0$, i.e. the magnitude decreases. Figure 3 shows the distribution of $\dot{\gamma}$ for the Newtonian fluid, at $t = 0.4$ and $t = 7.4$. Even
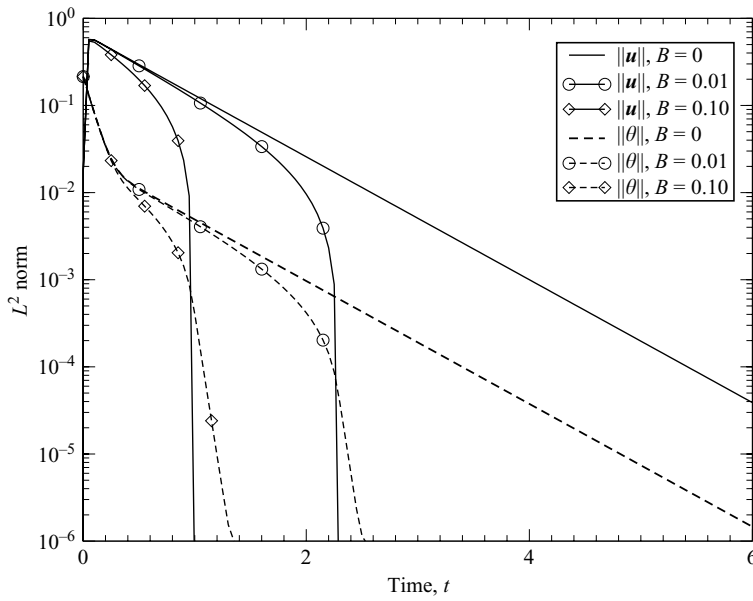
FIGURE 2. Evolution of $\|\boldsymbol{u}\|$ and $\|\theta\|$, for $Ra = 1500$, $Pr = 1$, at various Bingham numbers.
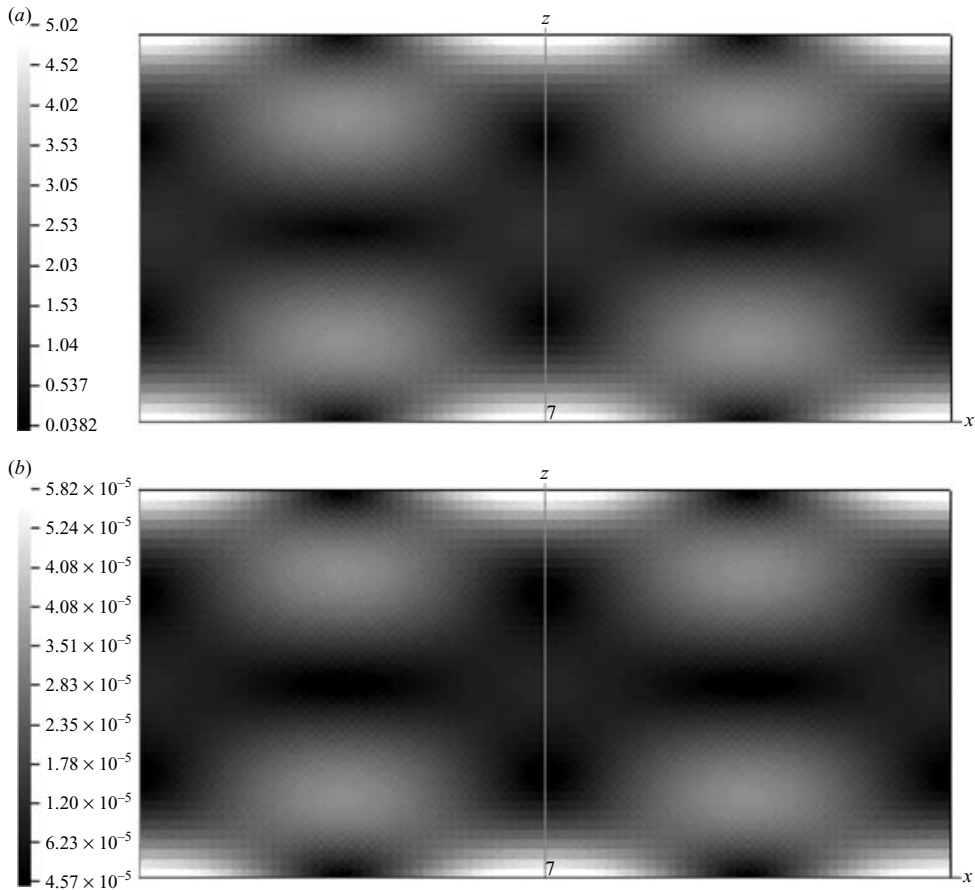

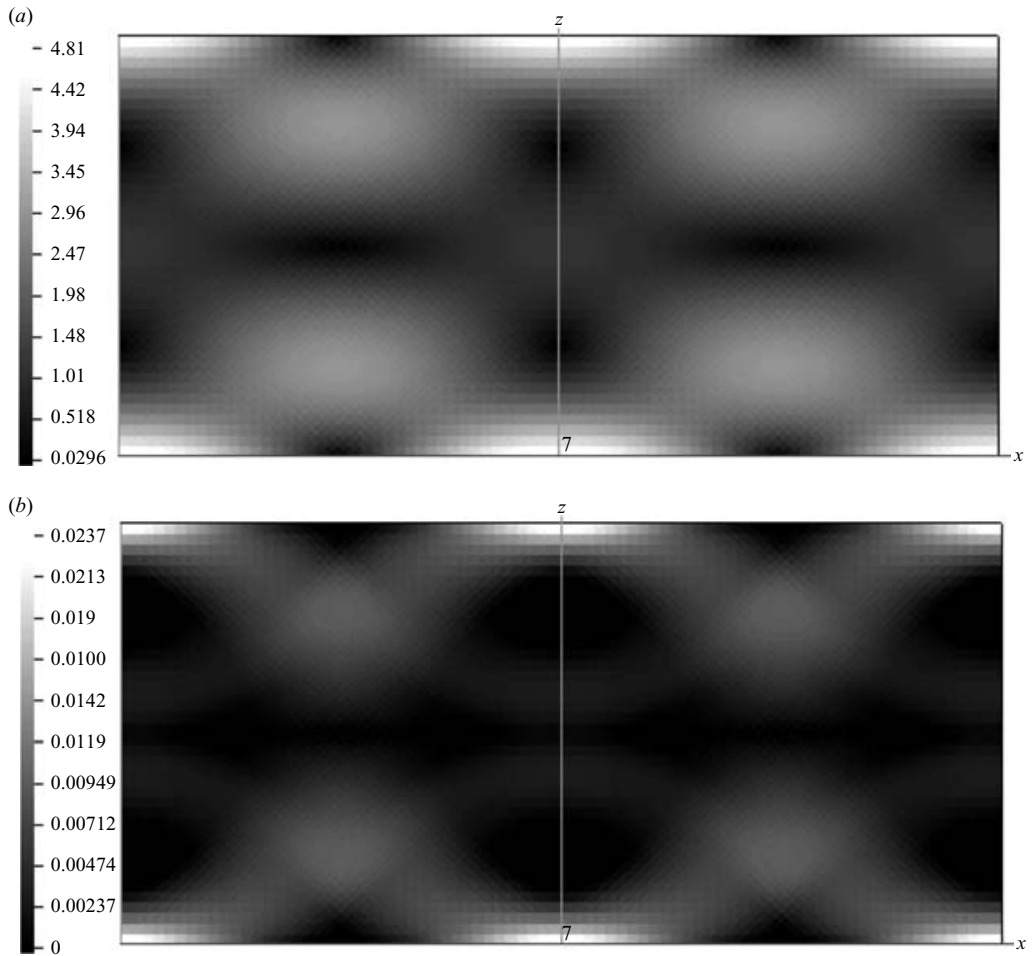FIGURE 3. Contours of $\dot{\gamma}$ for $Ra = 1500$, $Pr = 1$, Newtonian fluid: (*a*) $t = 0.4$; (*b*) $t = 7.4$.

FIGURE 4. Contours of $\dot{\gamma}$ for $Ra = 1500$, $Pr = 1$, Bingham fluid, $B = 0.01$: (*a*) $t = 0.4$; (*b*) $t = 2.25$.

though the rate of strain has decayed by five orders of magnitude, the distribution is very similar. We interpret this observation as the exponential decay of the least stable eigenmode of the linearized stability problem.

The Bingham fluid decays in a fundamentally different way. Figure 4 shows the distribution of $\dot{\gamma}$ for the Bingham fluid with $B = 0.01$, at $t = 0.4$ and $t = 2.25$. At $t = 0.4$, we can see in figure 2 that the velocity magnitude is similar to that for the Newtonian fluid, as is its distribution. In this regime, at large rates of strain, presumably the viscous dissipation terms are dominant and since $B \ll 1$, the yield stress has little effect. Therefore, we see a velocity distribution that resembles the modal Newtonian distribution. As $\|\boldsymbol{u}\| \to 0$, there is, however, a significant difference as the yield stress begins to dominate. At $t = 2.25$, unyielded regions have appeared, as shown explicitly in figure 5. The unyielded regions appear at the stagnation points and within the rotating cell. Note that these are not material surfaces: fluid flows into and out of the unyielded plug regions. Comparing with figure 4(*b*), we can see that there are also regions that are only just yielded. With the no-slip boundary conditions, purely rotational motion of the entire core does not appear possible. As
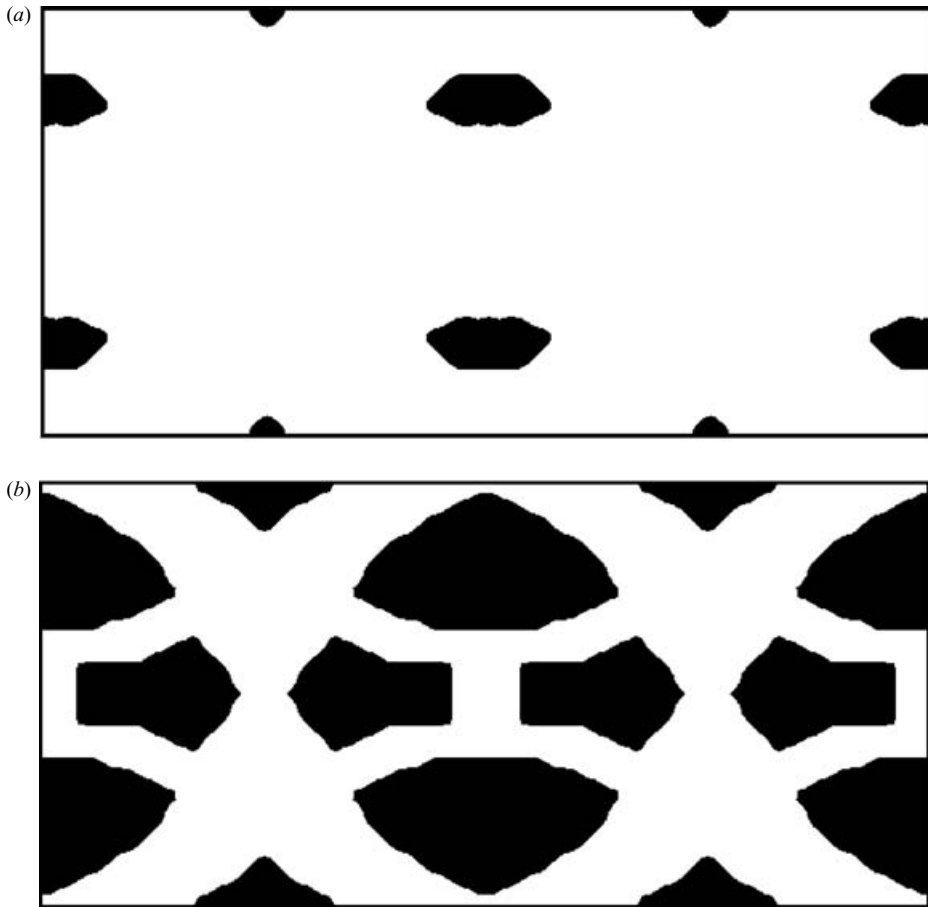
(*a*)

(*b*)

FIGURE 5. Growth of the unyielded regions as the flow stops, $Ra = 1500$, $Pr = 1$, $B = 0.01$: (*a*) $t = 2.25$; (*b*) $t = 2.28$. The flow stops at $t = 2.29$.

t increases, the unyielded plug regions grow very rapidly, concentrating the sheared fluid in progressively thin layers until the flow stops.

4.3. *Super-critical Rayleigh number: $Ra = 2000$*

For super-critical Rayleigh numbers, Theorem 3 indicates that we should expect conditional stability, with the bound depending on both Pr and B. In figure 1, we have seen that typically the conditional bound on the initial conditions increases with B and decreases with Pr and Ra. Consequently, we may verify the conditional hypothesis by varying any of a number of parameters. Here we focus on estimating a critical Bingham number for stability, with the initial condition (4.4) and for $k_x = 3$. After some iteration, we bracket the critical Bingham number as being between 0.571 and 0.572. Figure 6 shows the computed evolution of $\|u\|$ and $\|\theta\|$ for these values.

For the larger Bingham number, the fluid velocity and temperature decay back to the stratified steady state, in a qualitatively similar way to the sub-critical Rayleigh number cases (i.e. finite time decay of the velocity and exponential decay of the temperature, at two distinct rates). During the decay, we again see growth of the unyielded plug regions initiated both in the rotating cells and at the stagnation points between cells. Figure 7 shows the unyielded plug regions at $t = 3.98$.
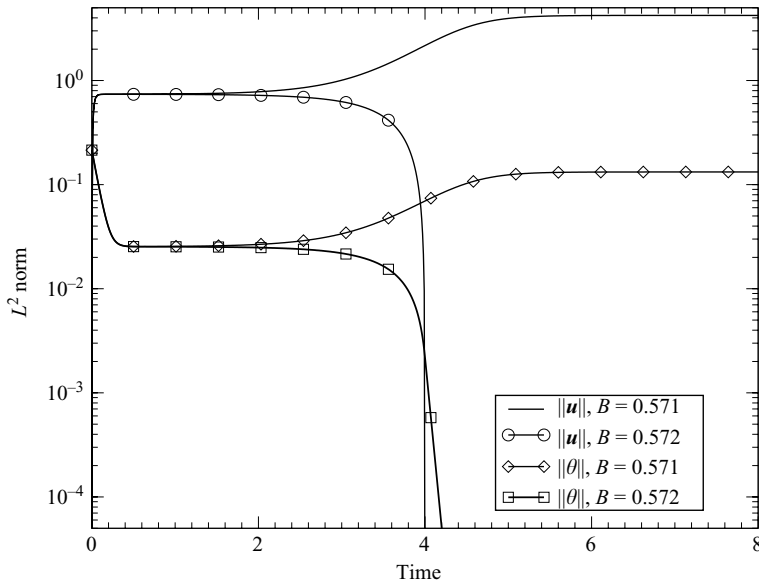
FIGURE 6. Evolution of $\|\boldsymbol{u}\|$ and $\|\theta\|$, for $Ra = 2000$, $Pr = 1$, at $B = 0.571$ and $B = 0.572$.
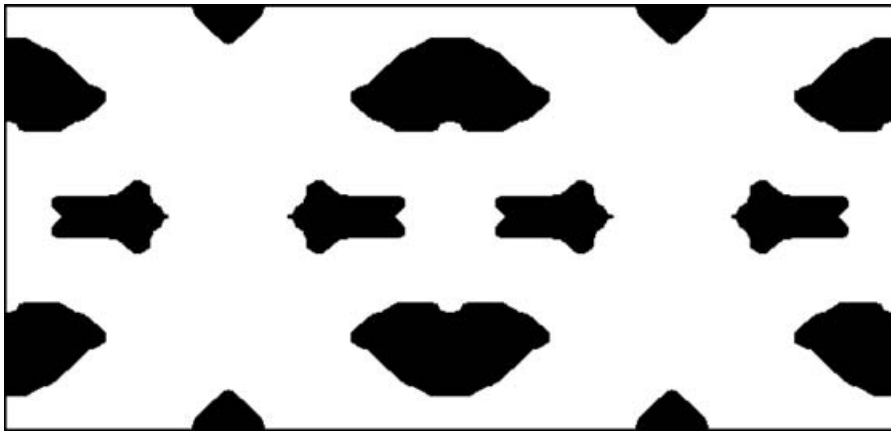

FIGURE 7. Unyielded regions of the stable solution for $Ra = 2000$, $Pr = 1$, $B = 0.572$ at $t = 3.98$.

For the lower Bingham number, the perturbation is not damped and stable secondary flow develops. Figure 8 shows the temperature field and streamlines at $t = 8$ for this case. The fluid has settled into a self-sustained steady cellular motion, reminiscent of the usual Rayleigh–Bénard cells found for a Newtonian fluid. To verify this, we have also computed the Newtonian fluid problem for $Ra = 2000$. Figure 9 shows the temperature and velocity components, at fixed x in the channel, and a comparison between the Newtonian and Bingham solutions. It appears that the steady convective patterns are in some sense very similar for the Newtonian fluid and for the Bingham fluid. What is surprising about this is first, that this is not obviously a small B perturbation of the Newtonian flow and also that we are far from criticality for the Newtonian flow.
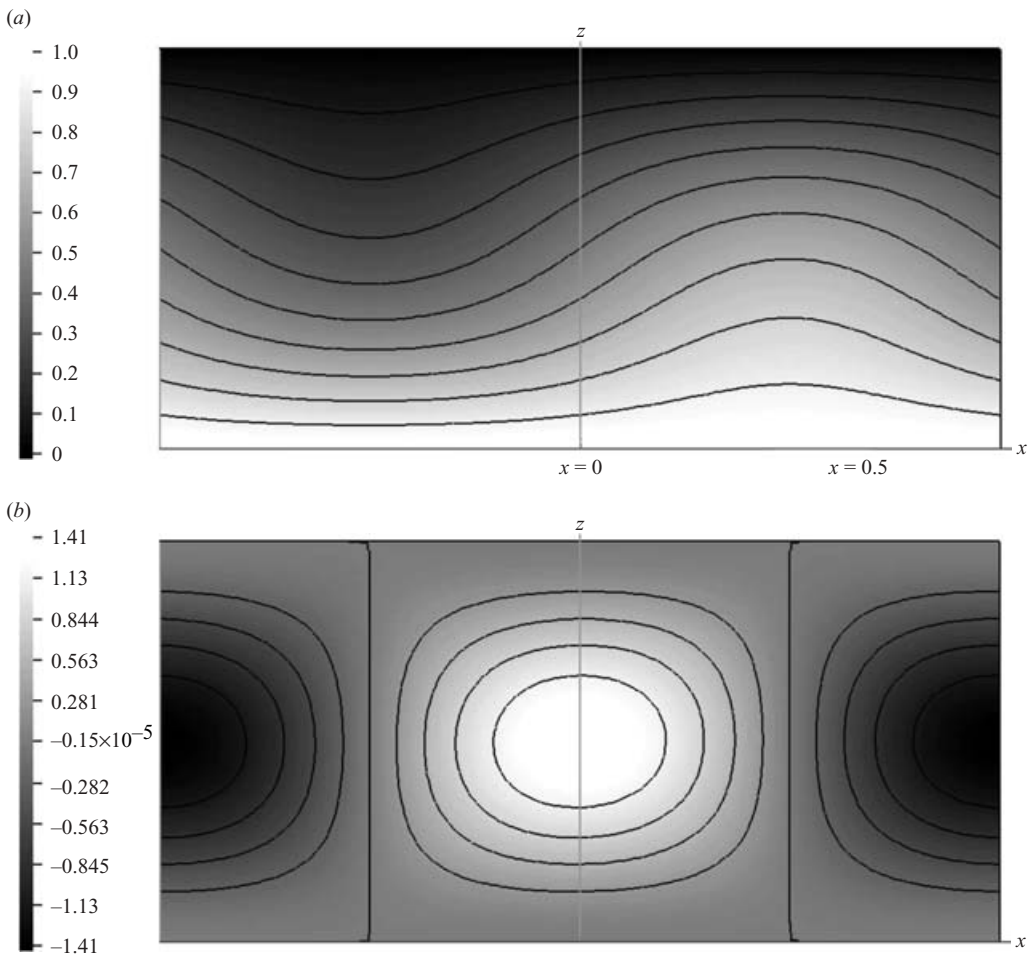
(*a*)

(*b*)

FIGURE 8. Unstable super-critical perturbation, $B = 0.571$, $Ra = 2000$, at $t = 8$: (*a*) temperature T; (*b*) streamlines.

On closer inspection however, we note that the differences in peak velocity in figure 9 are significantly larger than the temperature differences. We suggest that the streamlines of any sustained cellular motion would look qualitatively similar to the Newtonian cells and this is all we are observing.

4.4. *Marginal stability curves*

It is also possible to construct marginal stability curves using the computational solution. Such curves can be constructed with respect to any of the problem parameters. This is extremely time consuming to do and of limited value, in that the marginal stability curves are dependent on a particular initial condition, i.e. for the two-dimensional Bingham flow there is no guarantee that the cellular motions are attractors for all initial conditions that exceed the conditional stability bounds. An additional complication comes when computing solutions at small k_x. The transient solutions may diverge from stability whenever there is a stable subharmonic cellular motion, i.e. it is not possible to isolate one eigenmode as in the linear analysis. In practice, this means that a limited range of wavenumbers is considered.
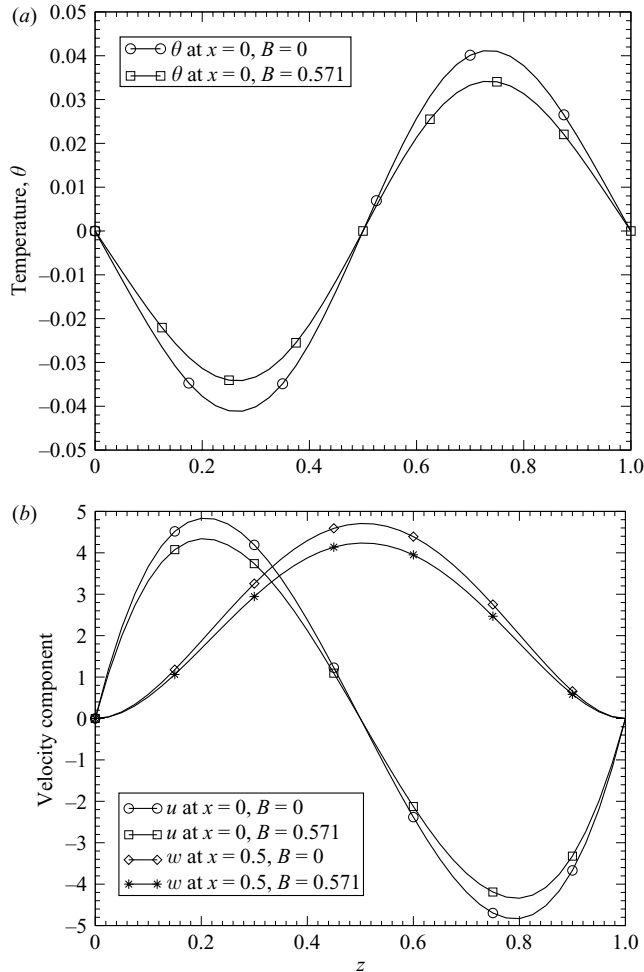
FIGURE 9. Comparison of Newtonian and Bingham ($B = 0.571$) cellular motions for $Ra = 2000$, at $t = 8$: (a) temperature T; (b) velocity components.

In figure 10, we show one example of a computed marginal stability curve. We have taken a relatively small $B = 0.05$, so that the Newtonian values may be used as an initial guess. The marginal stability curve is computed for the initial condition (4.4) and we take a range of wavenumbers about the Newtonian minimum. As expected, the Bingham curve is displaced above the Newtonian curve. The cellular motions when the critical values are exceeded are analogous to those reported above, i.e. the Bingham fluid cells resemble those for the Newtonian fluid, at the same wavelength.

A final comment concerning the supercritical cellular motions is that we have not observed unyielded plug regions in these flows, even when a range of wavenumbers is considered, as here.

5. Discussion and additional results

We have focused our analysis on perhaps the simplest non-trivial case, that of a two-dimensional plane channel with Dirichlet conditions satisfied on both top and bottom plates. The two principal differences with the Newtonian flow are: (i) finite
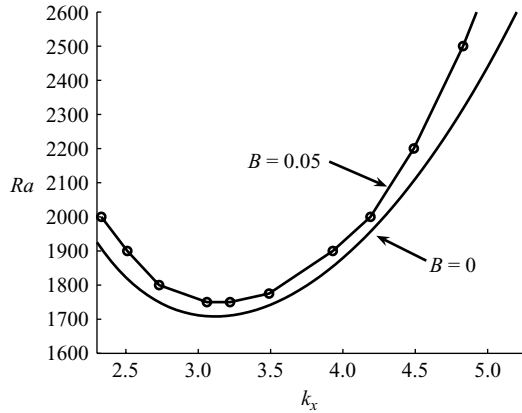
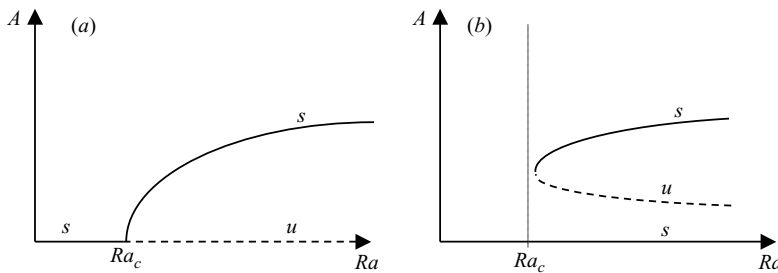FIGURE 10. Marginal stability curve at $B = 0.05$ for the initial condition (4.4).

FIGURE 11. Schematic of the bifurcation diagram with respect to Ra and solution amplitude A: (*a*) Newtonian, $B = 0$; (*b*) Bingham, $B > 0$.

time decay of the velocity field to zero, whenever the flow is stable; (ii) above the Newtonian critical Rayleigh number, $Ra_c = Ra_E$, we have a region of conditional stability for sufficiently small initial perturbations and arbitrarily high Ra, and for positive B.

The Newtonian system bifurcates at Ra_c. For $Ra > Ra_c$, the linear zero amplitude branch becomes unstable, but a stable upper branch of nonlinear cellular motions emerges, (see figure 11*a*). Our computations for $B > 0$ have also found stable cellular motions and our analysis suggests that the unstable branch is displaced upwards. Thus, for $B > 0$, the simplest plausible characterization of the bifurcation diagram would be as in figure 11(*b*).

The analysis, essentially as it is, generalizes in a straightforward way to the other usual boundary conditions, e.g. rigid–free and free–free. It is necessary only to replace Ra_E with the corresponding Newtonian energy stability limit. In order to achieve the finite time decay results, we must verify that the boundary conditions on the perturbation do not permit rigid-body motions. For the free–free boundary conditions, this means that linear motions of the fluid parallel to the walls must be discounted. A number of other results may also be derived, as we outline below.

5.1. *Heuristic analysis*

Although we have used rigorous methods, it is also possible to develop a heuristic analysis of the Rayleigh–Bénard paradigm for a yield stress fluid, by adapting classical

order of magnitude arguments for Newtonian fluids that can be found in various texts.

Consider a fluid particle of radius $\hat{R}$ in a stratified thermal field with vertical temperature gradient $\Delta\hat{T}/\hat{L}$. Suppose that the centre of the particle is $\delta\hat{T}$ hotter than the surrounding thermal field. Because of buoyancy, the particle moves upwards at speed $\hat{U}$. The particle loses heat via conduction to the surrounding fluid, at a rate $\propto \hat{K}\delta\hat{T}/\hat{R}^2$, but gains heat at a rate $\propto \hat{\rho}\hat{c}_p\hat{U}\Delta\hat{T}/\hat{L}$. Consequently, the particle centre remains hotter than its surroundings if

$$\hat{U} \geqslant \Lambda_1 \frac{\hat{\alpha}\delta\hat{T}\hat{L}}{\Delta\hat{T}\hat{R}^2},$$

for some dimensionless geometric constant Λ_1. Here $\hat{\alpha} = \hat{K}/(\hat{\rho}\hat{c}_p)$ is the thermal diffusivity of the fluid. On the other hand, the particle motion can only be sustained if the buoyancy of the particle, $\propto \hat{\rho}\hat{R}^3\hat{g}\hat{\beta}\delta\hat{T}$, exceeds the drag force on the fluid particle. In the case of a yield stress fluid, this amounts to:

$$\hat{\rho}\hat{R}^3\hat{g}\hat{\beta}\delta\hat{T} \geqslant \Lambda_2\hat{R}\hat{\mu}\hat{U} + \Lambda_3\hat{R}^2\hat{\tau}_Y,$$

for dimensionless geometric constants Λ_2, Λ_3. Scaling $\delta\hat{T}$ with $\Delta\hat{T}$, $\hat{R}$ with $\hat{L}$, and dividing through by the buoyancy force, we see that the motion is only self-sustaining if:

$$1 \geqslant \Lambda_4 \frac{\hat{\alpha}\hat{\mu}}{\hat{\rho}\hat{g}\hat{\beta}\Delta\hat{T}\hat{L}^3} + \Lambda_5 \frac{\hat{\tau}_Y}{\hat{\rho}\hat{g}\hat{\beta}\Delta\hat{T}\hat{L}} = \Lambda_4 \frac{1}{Ra} + \Lambda_5 B, \qquad (5.1)$$

for some dimensionless constants Λ_4, Λ_5. In the case where the fluid is stable, we would expect that the third dimensionless parameter, Pr, also influences the decay rate of perturbations to the basic state.

5.2. *Residual stresses*

As our steady base state we have considered a static temperature stratified fluid, and have made the additional assumption, in (2.6), that there are no residual stresses. Depending on how the fluid layer is formed there may indeed exist residual shear stresses in the static layer, (e.g. due to thermal stresses in a geophysical setting). If an estimate of the residual stresses τ_{ij}^R is available, the analysis presented can still be followed through, but with a reduced yield stress. Suppose that the static steady-state solution has residual stress τ_{ij}^R. Then we may assume that

$$\tau^R \leqslant B,$$

since the fluid is static. In place of the kinetic energy equation (2.7), we may straightforwardly derive:

$$\frac{1}{Pr}\frac{dH}{dt} = Ra\langle w\theta\rangle - B\langle\dot{\gamma}\rangle - \langle\dot{\gamma}^2\rangle + \langle\dot{\boldsymbol{\gamma}} : \boldsymbol{\tau}^R\rangle$$

$$\leqslant Ra\langle w\theta\rangle - \langle(B - \tau^R)\dot{\gamma}\rangle - \langle\dot{\gamma}^2\rangle. \qquad (5.2)$$

If say $\tau^R \leqslant \phi B$ for some $\phi \in (0, 1)$, then (5.2) is simply

$$\frac{1}{Pr}\frac{dH}{dt} \leqslant Ra\langle w\theta\rangle - \tilde{B}\langle\dot{\gamma}\rangle - \langle\dot{\gamma}^2\rangle,$$

where $\tilde{B} = (1 - \phi)B > 0$ is a reduced Bingham number. The preceding results are then valid with B replaced by $\tilde{B}$.

5.3. *Inclined channels*

A similar situation exists for inclined channels. Suppose that the channel walls are inclined at an angle ψ to the z-axis. The stratified temperature $T = 1 - z$ still provides a steady solution to the energy equation for static fluids. However, the stress and pressure must now satisfy:

$$0 = -\frac{\partial p}{\partial x} + \frac{\partial}{\partial x}\tau_{xx} + \frac{\partial}{\partial z}\tau_{xz} + Ra(1-z)\sin\psi,$$

$$0 = -\frac{\partial p}{\partial z} + \frac{\partial}{\partial x}\tau_{zx} + \frac{\partial}{\partial z}\tau_{zz} + Ra(1-z)\cos\psi.$$

We may observe that there is no solution to the above equations with zero shear stress, and consequently no static steady state for a Newtonian fluid. For a yield stress fluid the stress is indeterminate when unyielded, but we may find for example the following candidate solution:

$$\tau_{xx} = \tau_{zz} = 0, \quad p = \frac{Ra}{2}\left([2z - z^2]\cos\psi + x\sin\psi\right), \quad \tau_{xz} = \tau_{zx} = \frac{Ra\sin\psi}{2}\left(z - \tfrac{1}{2}\right)^2.$$

Slow flows of yield stress fluids do not yield if there is an admissible unyielded stress field. Thus, we see that provided

$$B > \tau \Rightarrow B > \frac{Ra\sin\psi}{4},$$

then a static steady solution exists. The static solution clearly has a residual stress, and we may then use any of the analytical results of this paper, replacing B with

$$\tilde{B} = B - \frac{Ra\sin\psi}{4}.$$

We note that this effectively introduces an extra Ra-number dependency into the stability results, interpreted in terms of B. In particular, for global asymptotic stability and finite time decay of the velocity, for a layer of fluid that can be oriented at any angle, it is necessary to have a fluid with

$$B > \frac{Ra_E}{4}.$$

5.4. *Extensions to three-dimensional stability*

In three dimensions, the energy equations (2.7) and (2.8) are still valid and at the outset it appears that all the results can be straightforwardly extended to three dimensions. However, this is not the case since the inequality (3.5) does not hold in three-dimensions. Although it is possible to bound a norm of $\boldsymbol{u}$ by $\langle\dot{\gamma}\rangle$, we may not bound the L^2 norm. The results in Témam & Strang (1980) give at best:

$$C_{TS,3}\|\boldsymbol{u}\|_{3/2} \leqslant \langle\dot{\gamma}\rangle, \tag{5.3}$$

for some $O(1)$ positive constant $C_{TS,3}$. This impacts the stability results in two ways. First, we can no longer ensure finite time decay of the velocity. Secondly, where our bounds are conditional on the size of perturbation, we must state conditions on $\|\theta\|_3$ in order to ensure decay of the energy (i.e. $\|\boldsymbol{u}\|$ and $\|\theta\|$). However, because $\|\theta\|_3$ is not bounded by $\|\theta\|$ (which is bounded by the decaying energy), the results are evidently weaker. We outline below those results that can be established.

5.4.1. *Linear stability*

Linear stability is always taken to mean that the perturbations are small in some norm. Here, we must simply be more specific about which norm. We suppose that $\|\theta\|_3$ is bounded for all t and let

$$\epsilon = \sup_t \|\theta\|_3(t). \qquad (5.4)$$

It follows that $\|\theta\| \sim O(\epsilon)$ and we assume also that $\|\boldsymbol{u}\| \sim O(\epsilon)$. Summing (2.7) and (2.8), using Holder's inequality and (5.3), we have

$$
\begin{aligned}
\frac{\mathrm{d}E}{\mathrm{d}t} &= (Ra+1)\langle w\theta \rangle - B\langle \dot{\gamma} \rangle - \langle \dot{\gamma}^2 \rangle - \langle |\nabla\theta|^2 \rangle \\
&\leqslant (Ra+1)\|\theta\|_3 \|w\|_{3/2} - BC_{TS,3}\|\boldsymbol{u}\|_{3/2} - \langle \dot{\gamma}^2 \rangle - \langle |\nabla\theta|^2 \rangle \\
&\leqslant [(Ra+1)\epsilon - BC_{TS,3}]\|\boldsymbol{u}\|_{3/2} - \langle \dot{\gamma}^2 \rangle - \langle |\nabla\theta|^2 \rangle.
\end{aligned}
$$

Thus, for sufficiently small $\epsilon < BC_{TS,3}/(Ra+1)$, we have exponential decay of the energy, (here $E = H/Pr + K$).

5.4.2. *Global stability*

Let $Ra_{E,3}$ be the energy Rayleigh number of the three-dimensional problem for a Newtonian fluid. Then as before, for $Ra < Ra_{E,3}$, $E(t) = H(t)/Pr + Ra_{E,3}K(t)$ decays according to

$$E(t) \leqslant E(0)\mathrm{e}^{-\lambda_1 t},$$

for some $\lambda_1 > 0$; see Theorem 2. Again we cannot establish finite time decay. For those flow configurations for which the Newtonian fluid becomes unstable first to a two-dimensional perturbation (and for which linear and energy stability limits coincide), we may also infer that there are no unstable three-dimensional perturbations to the Bingham problem, provided $Ra < Ra_E$ (since this would contradict the Newtonian results).

5.4.3. *Conditional stability*

As before, we consider an energy functional $E(t) = H(t)/Pr + Ra K(t)$, for which (2.7) and (2.8) give us:

$$
\begin{aligned}
\frac{\mathrm{d}E}{\mathrm{d}t} &= 2Ra_{E,3}\langle w\theta \rangle - \langle \dot{\gamma}^2 \rangle - Ra_{E,3}\langle |\nabla\theta|^2 \rangle + (Ra - Ra_{E,3})[2\langle w\theta \rangle - \langle |\nabla\theta|^2 \rangle] - B\langle \dot{\gamma} \rangle, \\
&\leqslant (Ra - Ra_{E,3})\left(2\|\boldsymbol{u}\|_{3/2}\|\theta\|_3 - \tilde{C}_P\|\theta\|^2\right) - BC_{TS,3}\|\boldsymbol{u}\|_{3/2}. \qquad (5.5)
\end{aligned}
$$

We see immediately that the energy $E(t)$ decays provided that the following uniform bound can be assumed on $\|\theta\|_3(t)$:

$$\sup_t \|\theta\|_3(t) < \frac{BC_{TS,3}}{2(Ra - Ra_{E,3})}. \qquad (5.6)$$

For this conditional stability limit, we do not have a decay rate estimate. Compare, however, with the linear stability result.

5.5. *Final remarks*

The stability results and analysis presented are illustrative of how to deal with coupled visco-plastic fluid systems. The methods are equally applicable to systems with concentration-dependent properties, double diffusive phenomena, etc. In Joseph (1976), a wide class of motionless Newtonian flows are identified, governed by the

Oberbeck–Boussinesq equations. Most of these flows could be extended to yield stress fluids and would be amenable to the type of analysis we have used. With reference to our discussion of inclined channels, the set of motionless steady flows that could be studied is considerably larger than for Newtonian fluids. Presumably, most of these flows would exhibit finite time decay of the velocity for sufficiently large yield stresses. The ability to control the yield stress rapidly and reversibly therefore suggests a means to switch on and off convective processes in mixing and heat transfer. These are exciting areas for future study.

In comparison to other stability studies in visco-plastic fluid flows, the results are a little different, since the base flow here is unyielded and static. Thus, there are no normal modes in the linear stability results and even the energy stability problem does not lead to a linear modal Euler–Lagrange problem. Although we suspect that the bounds we have derived are conservative, absence of these two classical avenues of attack leaves us without a clear method to compute the stability of the flow directly. Our indirect method, via two-dimensional transient simulation, is effective but also very slow to compute and not suitable for determining detailed parametric marginal stability curves. On the other hand, the computational results indicate many interesting features hidden from the analysis. In particular, flow behaviour as the stability limits are approached and study of how the fluid stops both appear worth studying further. Even though the wavenumber k_x does not enter explicitly into our analysis, preliminary computations indicate that the flow structures are sensitive to k_x, and this is also a topic for future study.

REFERENCES

ABU-RAMADAN, E., HAY, J. M. & KHAYAT, R. E. 2003 Characterization of chaotic thermal convection of viscoelastic fluids. *J. Non-Newtonian Fluid Mech.* **115**, 79–113.

BINGHAM, E. C. 1922 *Fluidity and Plasticity*, pp. 215–218. McGraw-Hill.

BIRD, R. B., DAI, G. C. & YARUSSO, B. J. 1983 The rheology and flow of visco-plastic materials. *Rev. Chem. Engng.* **1**, 1–70.

BIRD, R. B., ARMSTRONG, R. C. & HASSAGER, O. 1987 *The Dynamics of Polymeric Fluids. Volume I: Fluid Mechanics*, §2.2. Wiley.

DUVAUT, G. & LIONS, J. L. 1976 *Inequalities in Mechanics and Physics*, pp. 279–327. Springer.

EKELAND, I. & TÉMAM, R. 1976 *Convex Analysis and Variational Problems*, chap. 1, §5. North-Holland.

FORTIN, M. & GLOWINSKI, R. 1982 *Lagrangiens Augments*. Dunod.

FRIGAARD, I. A. 2001 Super-stable parallel flows of multiple visco-plastic fluids. *J. Non-Newtonian Fluid Mech.* **100**, 49–76.

FRIGAARD, I. A., HOWISON, S. D. & SOBEY, I. J. 1994 On the stability of Poiseuille flow of a Bingham Fluid. *J. Fluid Mech.* **263**, 133–150.

FRIGAARD, I. A. & NOUAR, C. 2003 On three-dimensional linear stability of Poiseuille flow of Bingham fluids. *Phys. Fluids* **15**, 2843–2851.

FRIGAARD, I. A., NGWA, G. & SCHERZER, O. 2003 On effective stopping time selection for visco-plastic nonlinear BV diffusion filters. *SIAM J. Appl. Math.* **63**, 1911–1934.

GEORGIEVSKII, D. V. 1993 Stability of two- and three-dimensional viscoplastic flows, and generalised Squire theorem. *Isv. Akad Naut SSR Mekh. Tverdogo Tela.* **28**, 117–123.

GLOWINSKI, R. 1984 *Numerical Methods for Nonlinear Variational Problems*. Springer.

GLOWINSKI, R., LIONS, J.-L. & TRÉMOLIÈRES, R. 1981 Numerical analysis of variational inequalities. North-Holland (trans. from French).

GRAEBEL, W. P. 1964 The hydrodynamic stability of a Bingham fluid in Couette flow. In *Proc. of International Symposium on 2nd Order Effects in Elasticity, Plasticity and Fluid Dynamics, Haifa, Israel, April 23–27, 1962*, (ed. M. Reiner & D. Abir), pp. 636–649. Jerusalem Academic Press.

HOWLE, L. E. 1997 Active control of Rayleigh–Bénard convection. *Phys. Fluids* **9**, 1861–1863.

HOWLE, L. E. 2000 The effect of boundary properties on controlled Rayleigh–Bénard convection. *J. Fluid Mech.* **411**, 39–58.

HUILGOL, R. R., MENA, B. & PIAU, J.-M. 2002 Finite stopping time problems and rheometry of Bingham fluids. *J. Non-Newtonian Fluid Mech.* **102**, 97–107.

JOSEPH, D. D. 1965 On the stability of the Boussinesq equations. *Arch. Rat. Mech. Anal.* **20**, 59–71.

JOSEPH, D. D. 1966 Nonlinear stability of the Boussinesq equations by the method of energy. *Arch. Rat. Mech. Anal.* **22**, 163–184.

JOSEPH, D. D. 1976 *Stability of Fluid Motions II*. Springer.

KHAYAT, R. E. 1995a Chaos and overstability in the thermal convection of viscoelastic fluids. *J. Non-Newtonian Fluid Mech.* **53**, 227–255.

KHAYAT, R. E. 1995b Non-linear overstability in the thermal convection of viscoelastic fluids. *J. Non-Newtonian Fluid Mech.* **58**, 331–356.

KHAYAT, R. E. 1995c Fluid elasticity and the transition to chaos in thermal convection. *Phys. Rev. E* **51**, 380–399.

KHAYAT, R. E. 1996 Chaos in the thermal convection of weakly shear-thinning fluids. *J. Non-Newtonian Fluid Mech.* **63**, 153–178.

KOSCHMIEDER, E. L. 1993 *Bénard Cells and Taylor Vortices*. Cambridge University Press.

LATCHÉ, J. C. & VOLA, D. 2004 Analysis of the Brezzi–Pitkaranta stabilized Galerkin scheme for creeping flows of Bingham fluids. *SIAM J. Num. Analysis* **42**, 1208–1225.

LANDRY, M. P., FRIGAARD, I. A. & MARTINEZ, D. M. 2005 Stability and instability of Taylor–Couette flows of a Bingham fluid. *J. Fluid Mech.* **560**, 321–353.

MARTINEZ-MARDONES, J., TIEMANN, R. & WALGRAEF, D. 1999 Convective and absolute instabilities in viscoelastic fluid convection. *Physica* A **268**, 14–23.

MARTINEZ-MARDONES, J., TIEMANN, R. & WALGRAEF, D. 2000 Rayleigh–Bénard convection in binary viscoelastic fluid. *Physica* A **283**, 233–236.

MÉTIVIER, C., NOUAR, C. & BRANCHER, J.-P. 2005 Linear stability involving the Bingham model when the yield stress approaches zero. *Phys. Fluids* **17**, 104–106.

MOSSOLOV, P. P. & MIASNIKOV, V. P. 1965 Variational methods in the theory of the fluidity of a viscous plastic medium. *J. Mech. Appl. Maths* **29**, 468–492.

MOSSOLOV, P. P., & MIASNIKOV, V. P. 1966 On stagnant flow regions of a viscous-plastic medium in pipes. *J. Mech. Appl. Maths* **30**, 705–717.

NOUAR, C. & FRIGAARD, I. A. 2001 Nonlinear stability of Poiseuille flow of a Bingham fluid; theoretical results and comparison with phenomenological criteria. *J. Non-Newtonian Fluid Mech.* **100**, 127–149.

NOUAR, C., DEVIENNE, R. & LEBOUCHÉ, M. 1994 Convection thermique pour un fluide de HerschelBulkley dans la région d'entrée d'une conduite. *Intl J. Heat Mass Trans.* **37**, 1–12.

OLDROYD, J. G. 1947 Two-dimensional plastic flow of a Bingham solid. *Proc. Camb. Phil. Soc.* **43**, 383–395.

PATEL, N. & INGHAM, D. B. 1994 Mixed convection flow of a Bingham plastic in an eccentric annulus. *Intl J. Heat Fluid Flow* **15**, 132–141.

PARK, H. M. & RYU, D. H. 2001a Rayleigh–Bénard convection of viscoelastic fluids in finite domains. *J. Non-Newtonian Fluid Mech.* **98**, 169–184.

PARK, H. M. & RYU, D. H. 2001b Hopf bifurcation in thermal convection of viscoelastic fluids within finite domains. *J. Non-Newtonian Fluid Mech.* **101**, 1–19.

PENG, J. & ZHU, K.-Q. 2004 Linear stability of Bingham fluids in spiral Couette flow. *J. Fluid Mech.* **512**, 21–45.

PRAGER, W. 1954 On Slow Visco-Plastic Flow. In *Studies in Mathematics and Mechanics*. Volume presented to Richard von Mises. Academic.

ROUND, G. F. & YU, S. 1993 Entrance laminar flows of viscoplastic fluids in concentric annuli. *Can. J. Chem. Engng* **71**, 642–645.

SANI, R. 1964 On the non-existence of subcritical instabilities in fluid layers heated from below. *J. Fluid Mech.* **20**, 315–319.

SINGER, J. & BAU, H. 1991 Active control of convection. *Phys. Fluids* A **3**, 2859–2865.

SOARES, M., SOUZA-MENDES, P. R. & NACCACHE, M. F. 1999 Heat transfer to viscoplastic materials flowing laminarly in the entrance region of tubes. *Intl J. Heat Fluid Flow* **20**, 60–67.

SOARES, M., NACCACHE, M. F. & SOUZA-MENDES, P. R. 2003 Heat transfer to viscoplastic materials flowing axially through concentric annuli. *Intl J. Heat Fluid Flow* **24**, 762–773.

TANG, J. & BAU, H. 1993 Stabilization of the no-motion state in Rayleigh–Bénard convection through the use of feedback control. *Phys. Rev. Lett.* **70**, 1795–1798.

TANG, J. & BAU, H. 1994 Stabilization of the no-motion state in the Rayleigh–Bénard problem. *Proc. R. Soc. Lond.* A **447**, 587–607.

TANG, J. & BAU, H. 1996 Stabilization of the no-motion state of a horizontal fluid layer heated from below with Joule heating. *Trans. ASME J. Heat Transfer* **117**, 329–333.

TÉMAM, R. & STRANG, G. 1980 Functions of bounded deformation. *Arch. Rat. Mech. Anal.* **75**, 7–21.

UKHOVSKII, M. R. & IUDOVICH, V. I. 1963 On the equations of steady state convection. *Prikl. Math. Mekh.* **27**, 295–300 (*J. Appl. Math. Mech.* **27**, 432–440).

VOLA, D., BOSCARDIN, L. & LATCHÉ, J. C. 2003 Laminar unsteady flows of Bingham fluids: a numerical strategy and some benchmark results. *J. Comput Phys.* **187**, 441–456.

VOLA, D., BABIK, F. & LATCHÉ, J. C. 2004 On a numerical strategy to compute gravity currents of non-Newtonian fluids. *J. Comput Phys.* **201**, 397–420.

WAGNER, B. A., BERTOZZI, A. L. & HOWLE, L. E. 2003 Positive feedback control of Rayleigh–Bénard convection. *Disc. Cont. Dyn. Sys.* B **3**, 619–642.